European Journal of Medicinal Chemistry 187 (2020) 111927

Contents lists available at ScienceDirect

European Journal of Medicinal Chemistry

journal homepage: http://www.elsevier.com/locate/ejmech

Research paper

Harmicines – harmine and cinnamic acid hybrids as novel antiplasmodial hits

Ivana Perković [a, **], Silvana Raić-Malić [b], Diana Fontinha [c], Miguel Prudêncio [c], Lais Pessanha de Carvalho [d], Jana Held [d], Tana Tandarić [e], Robert Vianello [e], Branka Zorc [a], Zrinka Rajić [a, *]

[a] University of Zagreb Faculty of Pharmacy and Biochemistry, A. Kovačića 1, 10000, Zagreb, Croatia
[b] University of Zagreb Faculty of Chemical Engineering and Technology, Marulićev trg 19, 10000, Zagreb, Croatia
[c] Instituto de Medicina Molecular João Lobo Antunes, Faculdade de Medicina, Universidade de Lisboa, Av. Prof. Egas Moniz, 1649-028, Lisboa, Portugal
[d] University of Tübingen, Institute of Tropical Medicine, Wilhelmstraße 27, 72074, Tübingen, Germany
[e] Rudjer Bošković Institute, Division of Organic Chemistry and Biochemistry, 10 000, Zagreb, Croatia

ARTICLE INFO

Article history:
Received 27 October 2019
Received in revised form
28 November 2019
Accepted 28 November 2019
Available online 29 November 2019

Keywords:
Harmine
Cinnamic acid
Triazole
Azide-alkyne cycloaddition
Antiplasmodial activity
*Pf*Hsp90
Molecular dynamics
P. berghei
P. falciparum

ABSTRACT

Harmicines constitute novel hybrid compounds that combine two agents with reported antiplasmodial properties, namely β-carboline harmine and a cinnamic acid derivative (CAD). Cu(I) catalyzed azide-alkyne cycloaddition was employed for the preparation of three classes of hybrid molecules: *N*-harmicines **6a-i**, *O*-harmicines **7a-i** and *N*,*O*-bis-harmicines **8a-g,i**. *In vitro* antiplasmodial activities of harmicines against the erythrocytic stage of *Plasmodium falciparum* (chloroquine-sensitive *Pf*3D7 and chloroquine-resistant *Pf*Dd2 strains) and hepatic stage of *P. berghei*, as well as cytotoxicity against human liver hepatocellular carcinoma cell line (HepG2), were evaluated. Remarkably, most of the compounds exerted significant activities against both stages of the *Plasmodium* life cycle. The conjugation of various CADs to harmine resulted in the increased antiplasmodial activity relative to harmine. In general, *O*-harmicines **7** exhibited the highest activity against the erythrocytic stage of both *P. falciparum* strains, whereas *N*,*O*-bis harmicines **8** showed the most pronounced activity against *P. berghei* hepatic stages. For the latter compound, molecular dynamics simulations confirmed binding within the ATP binding site of *Pf*Hsp90, while the weaker binders, namely **6b** and harmine, were found to be positioned away from this structural element. In addition, decomposition of the computed binding free energies into contributions from individual residues suggested guidelines for further derivatization of harmine towards more efficient compounds. Cytotoxicity screening revealed *N*-harmicines **6** as the least, and *O*-harmicines **7** as the most toxic compounds. Harmicines **6g**, **8b** and **6d** exerted the most selective action towards *Plasmodium* over human cells, respectively. These results establish harmicines as hits for future optimisation and development of novel antiplasmodial agents.

1. Introduction

Despite significant efforts towards the development of an antimalarial vaccine and of novel antiplasmodial therapeutics, malaria remains a life-threatening disease, affecting 219 million people and caused 435 000 fatal outcomes in 2017. Especially stressful is the fact that malaria kills more children under the age of five than any other infectious disease [1]. There are five species of *Plasmodium* that cause malaria in humans: *P. falciparum*, *P. vivax*, *P. ovale*, *P. malariae* and *P. knowlesi* [2]. *Plasmodium* parasites have a complex life cycle, which includes both a mammalian and an invertebrate host. Infection of the mammalian host includes an asymptomatic but obligatory hepatic developmental stage, and a symptomatic erythrocytic phase of infection [3]. Most antimalarial drugs act on the erythrocytic stage of infection, as is the case of artemisinin and its derivatives, chloroquine (CQ) and mefloquine [4]. On the other hand, primaquine (PQ), tafenoquine and bulaquine are the only registered drugs affecting hypnozoites, the latent or dormant parasite stages that may form in the liver following infection by

* Corresponding author.
** Corresponding author.
E-mail addresses: iperkovic@pharma.hr (I. Perković), zrajic@pharma.hr (Z. Rajić).

https://doi.org/10.1016/j.ejmech.2019.111927
0223-5234/

P. vivax and *P. ovale* parasites, which can cause malaria relapses [2,5,6]. Although artemisinin-based combination therapies are highly efficient in the treatment of *P. falciparum* malaria, several reasons urge the discovery of novel agents: *i*) up to date, there is no available vaccine against malaria, *ii*) measures for the vector control are not fully effective, and *iii*) the emergence of artemisinin-resistant *P. falciparum* strains [2,4,7]. Current drug discovery approaches include the development of analogues of existing drugs, resistance reversers and novel compounds with new mechanisms of action [3,8].

β-Carbolines, a large group of naturally occurring and synthetic indole alkaloids, could be a starting point for the discovery of novel antiplasmodial agents. Some of them, namely harmine, harmaline, harmalol and harman are present in the medicinal plants *Peganum harmala* and *Eurycoma longifolia*, used in the traditional Oriental medicine for the treatment of various diseases, including malaria [9,10]. Several *in vitro* and *in vivo* studies have corroborated the antiplasmodial activity of harmine [11,12]. In addition, naturally occurring manzamine alkaloids and 10-hydroxycanthin-6-one, as well as synthetic spiroindolones (spirotetrahydro-β-carbolines) (Fig. 1) are also β-carbolines with pronounced antiplasmodial activity [13–15]. One member of the spiroindolone class, cipargamin, is currently undergoing clinical trials for the malaria treatment [16].

To the best of our knowledge, only few publications report on the antiplasmodial activity of synthetic β-carboline derivatives, 1,2,3,4-tetrahydro- or 1-substituted β-carboline derivatives being the most described in the literature [17–26]. As the antiplasmodial potential of harmine derivatives is not fully explored, further research could lead to the identification and development of novel antiplasmodial agents, which might act alone or synergistically with other antiplasmodial drugs.

One method to identify new drug entities is to covalently combine two pharmacophores in one molecule, i.e. to prepare hybrid drugs. This concept has already been successfully employed in the preparation of compounds with pronounced antimalarial activity [4,27,28]. Available data also show that conjugation of the known 4- and 8-aminoquinoline antiplasmodial drugs to cinnamic acid (*trans*-3-phenyl-2-propenoic acid) and its derivatives (CADs) enhances their *in vitro* antiplasmodial activity [29,30]. Moreover, *N*-cinnamoyl chloroquine, primaquine, aminoacridines and 4-aminoquinoline derivatives have been reported as dual-acting antiplasmodial agents [29–32].

We have followed the hybrid drug concept to design harmicines **6**–**8**, which consist of harmine and cinnamic acid scaffolds. Here we present the synthesis and evaluation of the cytotoxicity and antiplasmodial activity of these compounds against the erythrocytic and hepatic stages of *Plasmodium*, and we discuss their possible mechanism of action.

2. Results and discussion

2.1. Chemistry

Cu(I) catalyzed azide-alkyne cycloaddition (CuAAC), also known as "click" chemistry, was applied to obtain the title compounds. CuAAC results with the introduction of a triazole ring, which is recognized as a bioisostere of amides [33]. The method requires azide and alkyne building blocks. To this end, we have prepared CADs-based azides **2a**-**i** and harmine-based alkynes **3**–**5** (Scheme 1). Azides **2** were obtained from CADs in a four-step procedure. In the first step, CADs were converted to the corresponding esters, followed by the reduction to alcohols **1a**-**i**. To avoid the reduction of the double bond present in CAD, mild reaction conditions with $LiAlH_4$ as the reducing agent were applied. Notably, we could not attain direct $LiAlH_4$-based reduction of cinnamic acid to the corresponding alcohol. Alcohols **1a**-**i** were further efficiently transformed to azides **2a**-**i** by the means of 2-azido-1,3-dimethylimidazolinium hexafluorophosphate (ADMP) in the presence of 1,8-diazabicyclo[5.4.0]undec-7-ene (DBU) [34]. Alkyne bearing compounds **3**–**5** were obtained by the alkylation of harmine or harmole with propargyl bromide, in the presence of NaH or Cs_2CO_3, respectively [35]. Alkylation of harmole with one equivalent of propargyl bromide in the presence of 1.4 equivalents of Cs_2CO_3 yielded predominantly *O*-propargyl derivative **4** and a small amount of *N*,*O*-bis derivative **5**. Propargylation of harmole with two equivalents of propargyl bromide and 2.8 equivalents of the same base led exclusively to product **5**. However, alkylation of harmine proceeded in the presence of the stronger base NaH.

Cinnamyl azides **2a**-**i** and harmine-based alkynes **3**–**5** served as starting materials for the CuAAC, which proved to be an efficient method for preparation of harmicines under mild reaction conditions and, in general, in good yields. Three types of derivatives were obtained, *N*-harmicines **6a**-**i**, *O*-harmicines **7a**-**i** and *N*,*O*-bis-harmicines **8a**-**g**,**i**. Altogether, we have prepared 26 harmicines, which were characterized by the standard spectroscopic/spectrometric methods (IR, MS, ^{13}C and ^{1}H NMR). High purity of the prepared compounds was assessed by the elemental analysis, with values for carbon, hydrogen, and nitrogen found to be within 0.4% of the calculated values for the proposed formula.

2.2. Biological evaluations

2.2.1. Antiplasmodial activity

Due to the expected antiplasmodial potential of the harmine-CADs hybrids **6**–**8**, their *in vitro* activity against the erythrocytic and hepatic stages of the *Plasmodium* life cycle was investigated towards the establishment of relevant structure-activity relationship (SAR).

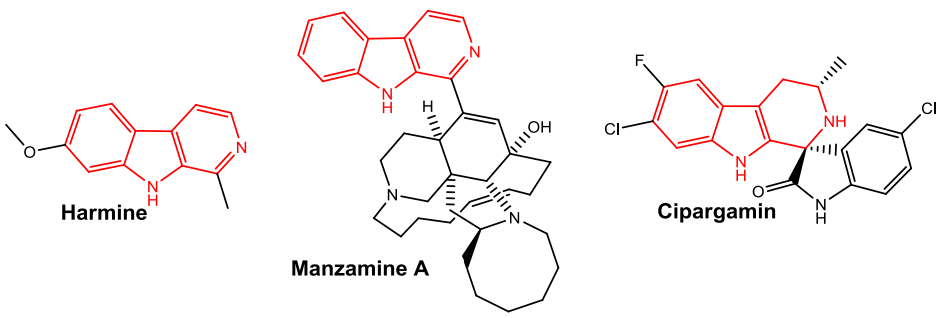

Fig. 1. β-Carbolines with antiplasmodial activity: harmine, manzamine A and cipargamin.

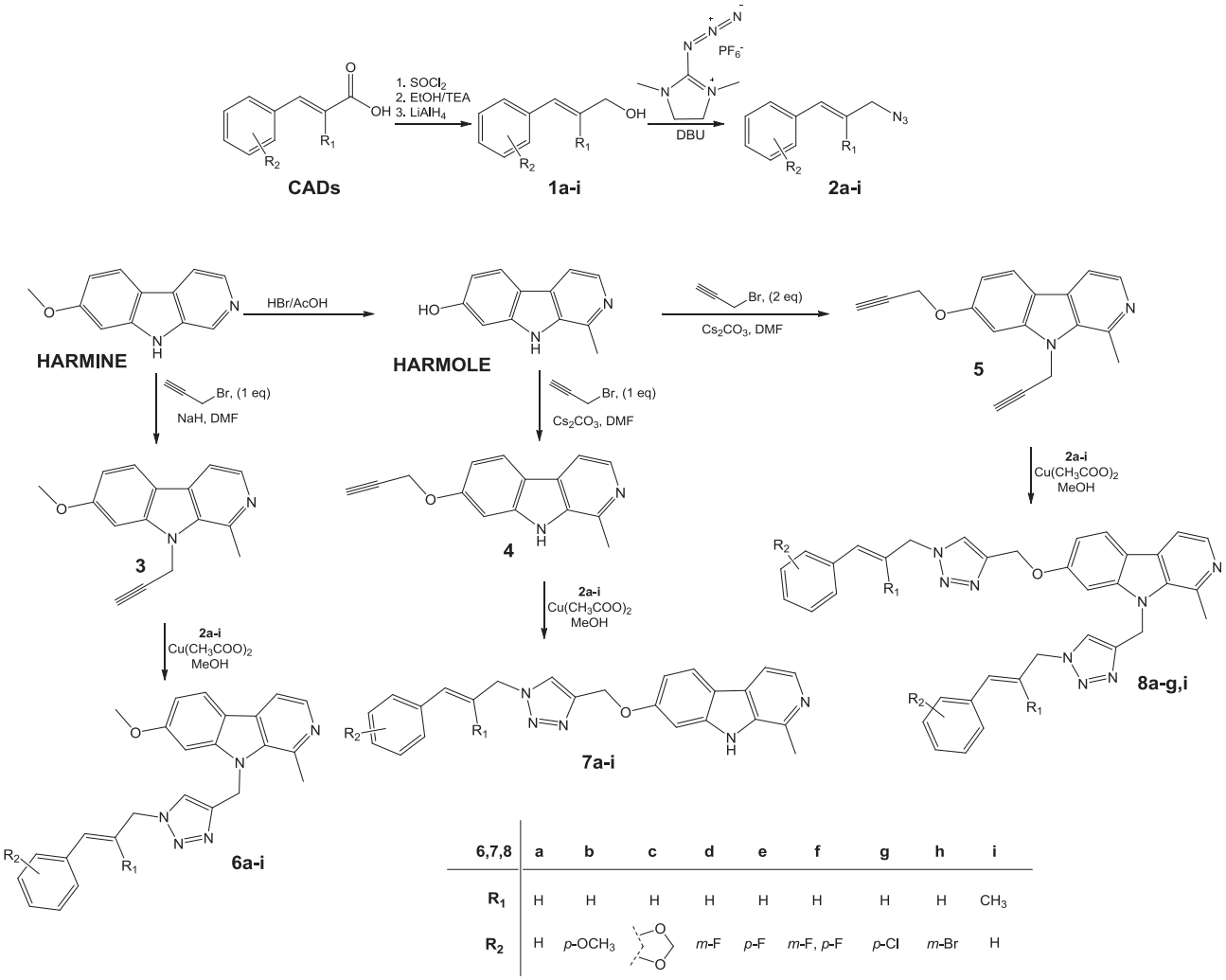

Scheme 1. Synthesis of harmicines **6**–**8**.

2.2.1.1. In vitro activity against P. falciparum erythrocytic stage. The activity of the compounds against the erythrocytic stage of *Plasmodium* life cycle was evaluated *in vitro* against two strains of *P. falciparum*, chloroquine-sensitive (*Pf*3D7) and chloroquine-resistant (*Pf*Dd2) strains, employing a previously described method [36–38] (Fig. 2 and Table 1).

The obtained data showed that harmicines exerted remarkable activity against both tested strains, higher than the parent compound harmine (in the most cases more than an order of magnitude higher). The activity against *Pf*3D7 and *Pf*Dd2 strains was in submicromolar and low micromolar concentrations, respectively. A detailed analysis of the activities of the homologues compounds

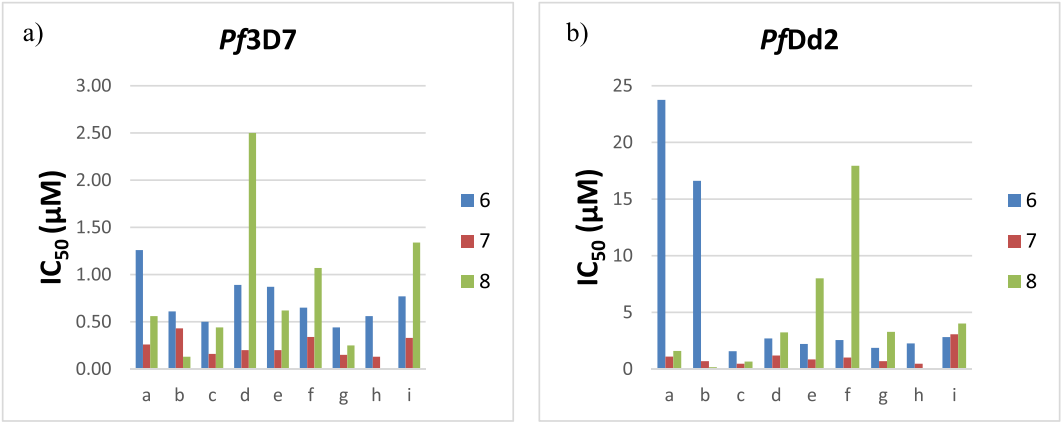

Fig. 2. Antiplasmodial activity of harmicines **6**–**8** against erythrocytic stage of a) chloroquine-sensitive (*Pf*3D7) and b) chloroquine-resistant (*Pf*Dd2) *P. falciparum* strains.

Table 1
In vitro screening of harmicines **6**–**8** against erythrocytic stage of *P. falciparum* (*Pf*3D7 and *Pf*Dd2 strains) and hepatic stages of *P. berghei*.

Compd.	IC_{50}[a] (μM)			log *P*[b]
	*Pf*3D7	*Pf*Dd2	P. bergei	
6a	1.26 ± 1.19[c]	23.76 ± 4.79[c]	2.62 ± 0.04[d]	4.26
6b	0.61 ± 0.51	16.61 ± 14.58	n.d.[e]	4.10
6c	0.50 ± 0.01	1.57 ± 0.28	n.d.	3.88
6d	0.89 ± 0.42	2.70 ± 1.21	n.d.	4.40
6e	0.87 ± 0.24	2.21 ± 0.13	n.d.	4.40
6f	0.65 ± 0.10	2.55 ± 0.77	n.d.	4.54
6g	0.44 ± 0.11	1.87 ± 0.58	1.12 ± 0.19	4.86
6h	0.56 ± 0.16	2.26 ± 0.33	1.10 ± 0.48	5.03
6i	0.77 ± 0.25	2.82 ± 1.80	n.d.	4.50
7a	0.26 ± 0.11	1.09 ± 0.28	n.d.	4.03
7b	0.43 ± 0.30	0.69 ± 0.10	n.d.	3.88
7c	0.16 ± 0.01	0.47 ± 0.07	n.d.	3.66
7d	0.20 ± 0.11	1.19 ± 0.36	n.d.	4.18
7e	0.20 ± 0.01	0.84 ± 0.17	n.d.	4.18
7f	0.34 ± 0.11	1.01 ± 0.09	n.d.	4.32
7g	0.15 ± 0.04	0.69 ± 0.26	n.d.	4.64
7h	0.13 ± 0.03	0.46 ± 0.13	n.d.	4.80
7i	0.33 ± 0.06	3.06 ± 2.47	0.66 ± 0.11	4.28
8a	0.56 ± 0.38	1.59 ± 1.19	n.d.	6.45
8b	0.13 ± 0.06	0.16 ± 0.02	0.4 ± 0.08	6.13
8c	0.44 ± 0.11	0.65 ± 0.57	n.d.	5.69
8d	2.50 ± 3.18	3.23 ± 1.88	n.d.	6.73
8e	0.62 ± 0.35	8.00 ± 4.71	n.d.	6.73
8f	1.07 ± 0.77	17.94 ± 16.46	n.d.	7.02
8g	0.25 ± 0.15	3.28 ± 1.56	n.d.	7.65
8i	1.34 ± 0.52	4.02 ± 1.87	n.d.	6.93
CQ[f]	0.003 ± 0.002	0.20 ± 0.10	n.d.	
Harmine	8.25 ± 2.83	>27.7	n.d.	
PQ[g]	n.d.	n.d.	8.4 ± 3.4	

[a] IC_{50}, the concentration of the tested compound necessary for 50% growth inhibition.
[b] log *P* – partition coefficient, calculated with Chemicalize.org software [39].
[c] Results represent mean ± SD, $n \geq 2$.
[d] Results represent mean ± SD, $n = 2$.
[e] n.d., not determined.
[f] CQ, chloroquine.
[g] PQ, primaquine.

from series **6**, **7** and **8** revealed O-substituted derivatives **7** as the most potent. In general, activity decreased following the pattern **7** > **8** > **6**, with one exception: in *p*-OCH_3 substituted series, **8b** was the most potent (**8b** > **7b** > **6b**). On the contrary, *N*,*O*-bis-harmicines with *m*-fluoro (**8d**), *m*,*p*-difluoro (**8f**) and α-methyl substituents exerted the weakest activity (**7d** > **6d** > **8d**, **7f** > **6f** > **8f, 7i** > **6i** > **8i**).

Comparison of IC_{50} values within the series of *O*-harmicines **7** showed that the substituents R_1 and R_2 on cinnamic scaffold had only minor effect, which was more pronounced for *N*-harmicines **6** and *N*,*O*-bis-harmicines **8**. Bulkiness of R_2 seemed to enhance *in vitro* activity. Further, replacement of hydrogen by its isostere fluorine in *m*- and *p*-positions in the cinnamic moiety yielded compounds with more pronounced antiplasmodial activity in the *N*-harmicine and *O*-harmicine, but not in the *N*,*O*-bis-harmicine series (for example **6d** > **6a**, **6e** > **6a**, **6f** > **6a**). On the other hand, substitution of hydrogen with methyl group in α-position in the cinnamic scaffold (R_1) led to the decreased antiplasmodial activity in the series of *O*-harmicines **7** and *N*,*O*-bis-harmicines **8** (**7a** > **7i**, **8a** > **8i**).

To assess the correlation between lipophilicity and activity, we have calculated log *P* values by employing the Chemicalize.org software (Table 1) [39]. Although the most active *O*-harmicines **7h** and **7g** are the most lipophilic ones in the series, IC_{50} values of other *O*-harmicines do not follow the same pattern. Lipophilicity does not seem to play an important role in the series of *N*-harmicines and *N*,*O*-bis-harmicines eighter.

The most active compounds against *Pf*3D7 strain were *N*,*O*-bis-harmicine **8b**, and *O*-harmicines **7c**, 7**g** and **7h** ($IC_{50} = 0.13–0.16$ μM), with *p*-OCH_3, methylenedioxy, *p*-Cl and *m*-Br substituents in the cinnamic part of the molecule, respectively. In addition, *N*,*O*-bis-harmicine **8b** exhibited the most pronounced activity towards both strains (IC_{50}(*Pf*Dd2) = 0.16 μM, IC_{50}(*Pf*3D7) = 0.13 μM).

2.2.1.2. In vitro activity against P. berghei hepatic stages. We further assessed the *in vitro* activity of harmicines against the hepatic stage of *Plasmodium* infection by employing the rodent *P. berghei* model, as previously described [40,41]. To assess their activity against *P. berghei* infection of Huh7 cells, the test compounds were initially screened at two concentrations, 1 and 10 μM (Fig. 3). Harmine was included as a positive control, whereas DMSO served as a negative control. Concomitantly, toxicity to the human hepatoma cell line (Huh7) was evaluated by cell confluency measurement. The 1 and 10 μM concentrations selected for each compound are typically employed in this kind of initial assessment [42–44], and enable the identification of compounds whose activity and toxicity warrant the subsequent determination of IC_{50} values.

The results showed that harmicines were active against hepatic stages of the *P. berghei* parasite. Remarkably, their activities were, in most cases, much higher than that of the parent compound, harmine. In this assay, *N*,*O*-bis-harmicines **8** exhibited the highest efficacy, followed by *N*-harmicines **6** and *O*-harmicines **7**. Notably, most of the compounds exerted moderate toxicity against Huh7 cells, at both tested concentrations.

The obtained IC_{50} values ranged between 0.4 and 2.62 μM (Table 1 and Fig. 4), which are up to 21 times lower than the IC_{50} of the reference drug PQ ($IC_{50} = 8.4 \pm 3.4$ μM) [42].

In conclusion, the conjugation of harmine with CADs *via* triazole linker led to derivatives with higher antiplasmodial activity than the parent compound harmine against both the erythrocytic and the hepatic stages of the *Plasmodium* infection. These findings are in agreement with the reported data for PQ- and CQ-CAD hybrids of the amide type [29,31,32], pointing to the importance of the cinnamic scaffold for the observed activity.

2.2.2. Cytotoxicity assay

Cytotoxicity against human liver hepatocellular carcinoma cell line (HepG2) was evaluated using the neutral red assay, as described previously [45] (Table 2). To assess the safety of harmicines, a selectivity index (SI) for each compound, as well as for the parent compound, was calculated as the fractional ratio between the IC_{50}s for HepG2 and *P. falciparum Pf*3D7 strain (Table 2). The obtained results show that *O*-harmicines were the most cytotoxic to HepG2 cells (SI = 2–77). Five *N*-harmicines (**6a**, **6b**, **6d**, **6g**, **6h**) and two *N*,*O*-bis-harmicines (**8b**, **8g**) did not exert significant cytotoxicity to HepG2 cells (SI > 100). Notably, the least cytotoxic *N*,*O*-bis-harmicines have substituents in *p*-positions in the CAD moiety, i.e. *p*-OCH_3 and *p*-Cl. In comparison to harmine (SI = 30), five *N*-harmicines **6**, four *O*-harmicines **7** and three *N*,*O*-bis-harmicines **8**, i.e. roughly 50% of all prepared harmicines, have more favourable selectivity indices, although SI for *O*-harmicines did not differ much from harmine. The least cytotoxic compound was **6g** (SI = 568), followed by **8b** (SI = 333) and **6d** (SI = 281). In conclusion, SI values depended on both the type of harmicines and the substituent in the CAD region.

2.3. Molecular dynamics

Molecular dynamics (MD) simulations were performed in order to offer more insight into the binding of *N*,*O*-bis-harmicine **8b**, elucidated as one of the most promising lead structures for the

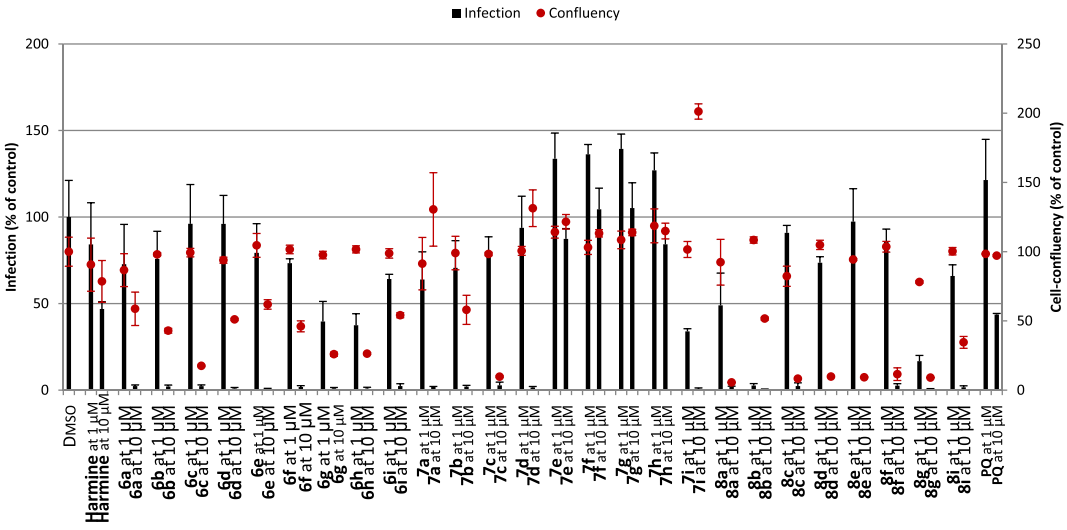

Fig. 3. *In vitro* activity against *P. berghei* liver stages of *N*-harmicines **6a-i**, *O*-harmicines **7a-i** and *N,O*-bis-harmicines **8a-g,i** at 1 and 10 μM concentrations. Total parasite load (infection scale, bars) and cell viability (cell confluency scale, dots) are shown. Results were normalized to the negative control, DMSO, and are represented as mean ± SD, $n = 1$.

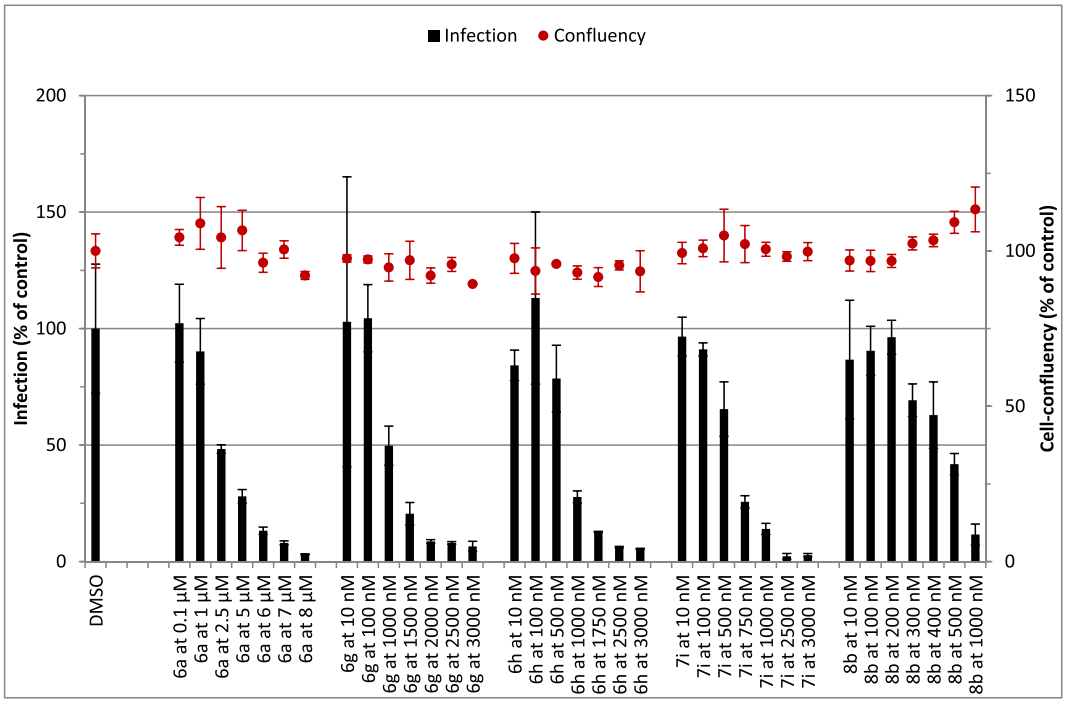

Fig. 4. Dose-dependent response of the selected harmicines against *P. berghei* hepatic stages. The determined IC_{50} values are presented in Table 1.

future design strategies, towards *P. falciparum* heat shock protein 90 (*Pf*Hsp90), and to reveal specific interactions governing the binding. These results will be discussed in comparison with a smaller compound **6b** and the parent compound harmine in order to evaluate the suitability of different substitution patterns for the biological activity. Specifically, **6b** combines the *N*-arm of **8b** and the *O*-arm of harmine, while maintaining a low cytotoxicity, being a good model to inspect the importance of the O-substitution on the activity. The choice of harmine is prompted by the fact that it was identified as a selective inhibitor of *Pf*Hsp90, which is essential for the erythrocytic development of *Plasmodium* [46,47].

*Pf*Hsp90 exists as a homodimer with three domains, namely the N-terminal GKHL ATP-binding domain (found also in type II topoisomerases, CheA-family histidine kinases, and the MutL DNA repair factor), a middle domain that supports ATP turnover (and which is also shared with type II topoisomerases and MutL), and a C-terminal dimerization domain [48,49]. It has been shown that ATP binding pocket of the N-terminal domain represents a crucial site where antiplasmodial agents bind and exert their activity [50,51].

The calculated binding free energies (ΔG_{BIND}) for the selected compounds are presented in Table 3, together with their decomposition into contributions from individual residues. The specific residues considered for the analysis are selected to list those established to be responsible for the binding of ATP within the ATP binding pocket (Asn37, Asp79, Arg98, Phe124) [50,51], and all those

Table 2
IC_{50} values for harmicines **6**–**8** tested *in vitro* on HepG2 cell line and calculated selectivity indices.

Compd.	IC_{50} (μM) HepG2	SI[a]	Compd.	IC_{50} (μM) HepG2	SI[a]
6a	>250	198	**7e**	2.19 ± 0.82	11
6b	>120	197	**7f**	0.74 ± 0.29	2
6c	8.78 ± 0.79	18	**7g**	8.80 ± 4.33	59
6d	>250	281	**7h**	2.86 ± 1.10	22
6e	8.88 ± 3.04	10	**7i**	25.32 ± 3.96	77
6f	9.75 ± 4.23	15	**8a**	8.59 ± 3.31	15
6g	>250	568	**8b**	43.33 ± 5.09	333
6h	56.63 ± 5.06	101	**8c**	36.14 ± 23.77	82
6i	11.87 ± 2.40	15	**8d**	6.01 ± 2.14	2
7a	9.67 ± 4.92	37	**8e**	12.14 ± 2.03	20
7b	5.37 ± 2.18	12	**8f**	10.99 ± 2.50	6
7c	5.60 ± 3.87	35	**8g**	29.03 ± 17.61	116
7d	3.11 ± 0.48	16	**8i**	24.97 ± 8.93	19
			Harmine	>250	30

[a] SI, selectivity index, ratio between IC_{50} (*Pf*3D7) and IC_{50} (HepG2).

Table 3
Calculated total binding free energies (ΔG_{BIND}) from molecular dynamics trajectories using MM-GBSA approach, and their decomposition on a per-residue basis for selected residues (all values in kcal mol^{-1}).

Compd.	6b	8b	harmine
Total ΔG_{BIND} (kcal mol^{-1})	−39.0	−40.1	−7.5
Asn37	0.00	−1.09	0.00
Asp79	0.01	0.31	0.00
Arg98	0.01	−0.06	0.00
Phe124	0.00	−0.86	0.00
Met84	0.00	−1.63	0.00
Asn92	0.01	−1.43	0.00
Ala41	0.00	−1.27	0.00
Ile82	0.00	−1.22	0.00
Thr101	−0.16	−1.06	−0.01
Lys44	0.01	−1.00	0.00
Asn91	0.00	−0.95	0.00
Ala103	−0.06	−0.79	−0.02
Ala38	0.00	−0.61	0.00
Lys102	−0.03	−0.59	−0.34
Leu93	0.00	−0.56	0.00
Thr171	0.00	−0.55	0.00
Ser99	−0.05	−0.55	0.00
Ile173	0.00	−0.51	−0.01
Arg169	0.00	0.05	0.00
Ser2	0.00	0.06	0.05
Asp141	0.00	0.07	0.00

with contributions higher than −0.50 and lower than 0.05 kcal mol^{-1} for the potent **8b**. In other words, data in Table 3 denote residues being most and least responsible for the binding of **8b** to *Pf*Hsp90.

Our data show that ΔG_{BIND} values for all three systems are negative and indicate favourable binding. Still, the value for **8b** is the most exergonic at −40.1 kcal mol^{-1}, demonstrating its better positioning within the binding site than **6b**, for which the calculated value assumes ΔG_{BIND}(**6b**) = −39.0 kcal mol^{-1}. These values are strongly in line with a trend in the measured IC_{50} values (Table 1), being IC_{50}(**8b**) = 0.13 μM and IC_{50}(**6b**) = 0.61 μM, respectively. Even more importantly than absolute values, a relative difference between the calculated binding free energies of $\Delta\Delta G_{BIND}$(**8b**−**6b**) = 1.1 kcal mol^{-1} is in excellent agreement with a value of 0.9 kcal mol^{-1} predicted from a difference in the measured IC_{50} values. This notion provides strong support to the obtained computational data and lends credence to the derived conclusions. On the other hand, relative to those two derivatives, harmine reveals poor binding properties as its binding free energy is much lower, ΔG_{BIND}(harmine) = −7.5 kcal mol^{-1}, being consistent with significantly higher IC_{50} value of 8.25 μM (Table 1). Moreover, although a relationship between IC_{50} and ΔG_{BIND} values is not so straightforward, the IC_{50} value measured for harmine roughly translates to a binding energy of −6.9 kcal mol^{-1}, which again confirms the validity of our computational setup and nicely ties our computational results with experiments.

Interestingly, although the calculated ΔG_{BIND} values for **8b** and **6b** are only vaguely different, their decomposition into contributions from specific residues reveals quite opposite trends. By analysing data in Table 3, it becomes evident that **8b** is positioned within the ATP binding site of *Pf*Hsp90, as it forms significant interactions with residues that define this site. This holds in particular for Asn37 and Phe124, where the obtained contributions are −1.09 and −0.86 kcal mol^{-1}. The overall effect of these two residues is somewhat reduced by the unfavourable effect of Asp79, which is overcome by the contribution of several other residues listed in Table 3 that promote the binding, and which are positioned close to the ATP binding site. These observations support the binding of **8b** to *Pf*Hsp90 within the ATP binding site and signifies the importance of this structural element as a druggable target. A close inspection of the MD trajectory reveals that the methoxy substituent (R_2 = *p*-OMe), placed on the phenyl ring attached onto the *O*-site of harmine, causes steric interference with Asp79, providing an explanation for the negative contribution of this residue to the binding of **8b**. An analysis of the evolution of distances between the carbon atom of the mentioned methoxy group and the carbon atom of the carboxylic group on Asp79 (Fig. 5) reveals that for more than half of the simulation time, these distances are found below 5 Å, which indicates their vicinity during the simulation. It follows that substituents other than the methoxy group introduced in **8b** (R_2 = −OMe), which would be able to form a stabilizing hydrogen bonding with the COO^- group on Asp79, could likely work towards further increasing the binding of such conjugates, which will be tackled in our future research. This observation also highlights the importance of the *O*-site of harmine for the *Pf*Hsp90 enzyme inactivation, since our MD simulations show that substituents at the *N*-site are predominantly stacking above the harmine aromatic core and do not show specific interactions with the protein. This insight might provide valuable information for the further derivatizations of harmine.

Additionally, our results demonstrated **6b** to be a slightly poorer binder than **8b**. Although **6b** is much smaller, it is not favourably positioned within the ATP binding site, and is pushed somewhat

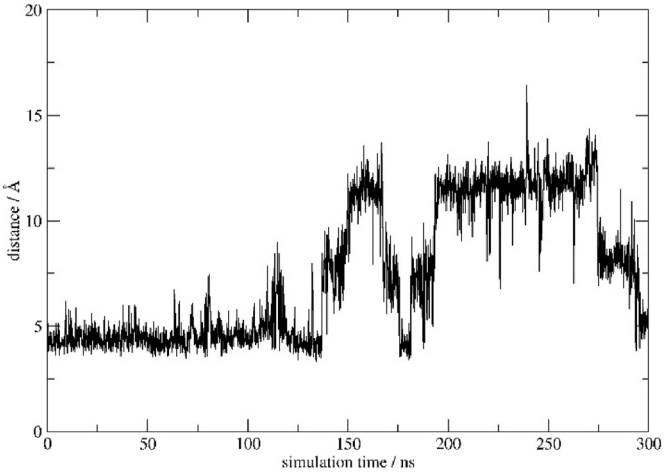

Fig. 5. Evolution of the C(*p*-OMe, **8b**)–C(COO^-, Asp79) distances during 300 ns of MD simulations. Average distance is 7.45 Å, clearly indicating their vicinity during the entire simulation.

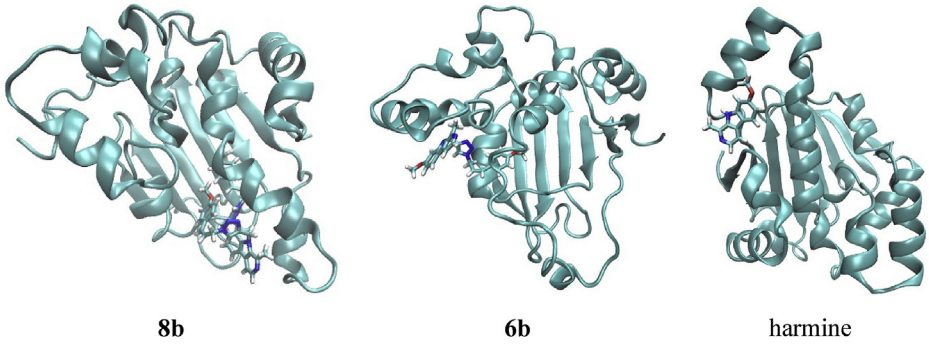

Fig. 6. Different binding positions of **8b**, **6b** and harmine for *Pf*Hsp90 as obtained through MD simulations.

away from it (Fig. 6) (there is practically no interactions with any of the four residues that define this cavity). As seen in Table 3, **6b** forms favourable interactions with Thr101, Ala103, Ser99, and Lys102, as well as with Pro204 (-0.85 kcal mol^{-1}), Ala107 (-0.49 kcal mol^{-1}), Val194 (-0.42 kcal mol^{-1}), and Ile205 (-0.42 kcal mol^{-1}), being the only four residues with favourable contributions exceeding -0.4 kcal mol^{-1}. The same qualitative conclusion can also be achieved for harmine, which is a much weaker binder than **8b** and **6b**. In addition, data in Table 3 clearly suggest that harmine binds outside the ATP binding site (Fig. 6). There are only two residues with individual contributions higher than -0.4 kcal mol^{-1} that promote the binding, namely Ile20 (-0.17 kcal mol^{-1}) and Met16 (-0.44 kcal mol^{-1}), being in agreement with its low affinity for *Pf*Hsp90.

In concluding this part, let us mention that calculated ΔG_{BIND} values are in good agreement with values predicted from the IC_{50} measurements, while their decomposition to contributions from individual protein residues signifies that **8b** strongly binds within the ATP binding site. Weaker binders, **6b** and, especially, harmine, are positioned further away from this structural element.

3. Conclusions

We have designed, synthesized and evaluated *in vitro* antiplasmodial activity and cytotoxicity of three classes of harmicines, hybrid molecules of alkaloid harmine and cinnamic acid derivatives connected *via* triazole linker. *N*-harmicines **6**, *O*-harmicines **7** and *N*,*O*-bis-harmicines **8** were prepared from cinnamyl azides and harmine-based alkynes, using Cu(I) catalyzed cycloaddition.

Most compounds exhibited pronounced antiplasmodial activity against the erythrocytic stage of *P. falciparum*, higher than the parent compound harmine, with IC_{50} values in submicromolar or one-digit micromolar concentrations for CQ-sensitive *Pf*3D7 and CQ-resistant *Pf*Dd2 strain, respectively. In this assay, the activity followed the pattern **7** > **8** > **6**. However, the evaluation of antiplasmodial activity against the hepatic stages of *P. berghei* revealed hybrids **8** as the most active, followed by harmicines **6** and **7**. In general, harmicines exerted higher activity than harmine, which, in some cases, was also higher than the reference drug primaquine. To the best of our knowledge, this is the first report of the activity of harmine and its derivatives against the hepatic stages of *Plasmodium*.

Molecular dynamics simulations suggest that *N*,*O*-harmicine **8b** strongly binds within the ATP binding site on *Pf*Hsp90, a potential target of antiplasmodial agents. As a prospective extension of this work, a replacement of the introduced methoxy group in **8b** with a substituent that would be able to form stabilizing hydrogen bonding interactions with Asp79 was identified as a viable strategy towards even more efficient compounds.

Cytotoxicity assay employing the HepG2 cell line identified *N*,*O*-bis-harmicines **8** as the least, and *O*-harmicines **7** as the most toxic. Substituents on cinnamic scaffold had minor effect on both activity and cytotoxicity within the series of *O*-harmicines **7**, and stronger effect in the other two series. The highest selectivity indices were obtained for **6g** (SI = 568), followed by **8b** (SI = 333) and **6d** (SI = 281), which makes them suitable candidates for the future optimisation and development of effective antiplasmodial agents.

4. Materials and methods

4.1. Chemistry

4.1.1. General information

Melting points were determined on a Stuart Melting Point Apparatus (Barloworld Scientific, UK) and were uncorrected. IR spectra were recorded on a FTIR PerkinElmer Paragon 500 spectrometer (PerkinElmer, Waltham, MA, USA). ^{1}H and ^{13}C NMR spectra were recorded on a Bruker Avance III HD operating at 300 or 400 MHz for the ^{1}H and 75, 101 or 151 MHz for the ^{13}C nuclei (Bruker, Billerica, MA, USA). Samples were measured in DMSO-d_6 solutions at 20 °C in 5 mm NMR tubes. Chemical shifts (δ) are reported in parts per million (ppm) using tetramethylsilane (TMS) as reference in the ^{1}H and DMSO residual peak as reference in the ^{13}C spectra (39.52 ppm). Coupling constants (J) are reported in hertz (Hz). Mass spectra were recorded on HPLC-MS/MS (HPLC, Agilent Technologies 1200 Series; MS, Agilent Technologies 6410 Triple Quad, Santa Clara, CA, USA). Mass determination was performed using electrospray ionization (ESI) in a positive mode. Elemental analyses were performed on a CHNS LECO analyzer (LECO Corporation, St. Joseph, MI, USA). Analyses indicated by the symbols of the elements were within ±0.4% of their theoretical values. All compounds were routinely checked by TLC with Merck silica gel 60F-254 glass plates using the following solvent systems: cyclohexane/ethyl acetate/methanol (3:1:0.5, 3:1:0.75, 1:1:0.3, 1:1:0.5), cyclohexane/ethyl acetate (2:1, 9:1), dichloromethane/methanol (9.7:0.3, 9.5:0.5 and 7.5:2.5). Spots were visualized by short-wave UV light and iodine vapour. Column chromatography was performed on silica gel (0.063–0.200 mm), with the same eluents used for TLC. All chemicals and solvents were of analytical grade and purchased from commercial sources. CADs were purchased as predominantly *trans* stereoisomers (≥99%). 4-Methoxy-cinnamic acid, 3,4-(methylenedioxy)cinnamic acid, 4-chlorocinnamic acid, 3-fluorocinnamic acid, 4-fluorocinnamic acid, cinnamyl alcohol, α-methyl-*trans*-cinnamaldehyde, harmine, ADMP and DBU were purchased from Sigma-Aldrich (St. Louis, MO, USA). 3,4-Difluorocinnamic acid and 3-bromocinnamic acid were purchased from TCI Chemicals (Tokyo, Japan). Harmole was prepared according to the modified literature procedure from harmine using

HBr/glacial acetic acid mixture, under the MW irradiation [52].

4.1.2. General procedure for the synthesis of ethyl cinnamoate derivatives

A solution of CAD (0.3 mmol), thionyl chloride (1.1 mL, 1.78 g, 1.5 mmol) and two drops of DMF in dry toluene was stirred at r.t. for 1 h. The solvent was evaporated. The acyl chloride residue was dissolved in dry toluene, evaporated again and dissolved in dry dichloromethane (DCM). A solution of TEA (0.419 mL, 0.304 g, 0.3 mmol) in absolute EtOH was added dropwise to a DCM solution of acyl chloride and stirred at r.t. for 1 h. The solvents were evaporated under reduced pressure. The residue was dissolved in 30 mL ethyl acetate/water mixture (1:1). The organic layer was extracted with water (2 × 30 mL), dried over anhydrous sodium sulfate and evaporated under reduced pressure to yield a crude product as an oily substance, which precipitated with time. Obtained esters were used in the next step without further purification.

*4.1.3. General procedure for the synthesis of cinnamyl alcohols (**1b-i**)*

To a solution of α-methyl-*trans*-cinnamaldehyde (0.042 g, 0.29 mmol) or corresponding ester (0.29 mmol) in dry diethyl ether, $LiAlH_4$ (0.5 or 1.0 mmol) was added under argon atmosphere at −5 °C. The reaction was stirred for 1.5 h at −5 °C. The reaction was then quenched with water (20 mL). The organic layer was extracted with diluted HCl (1%) (2 × 20 mL) and water (2 × 20 mL), dried over anhydrous sodium sulfate and evaporated under the reduced pressure. After purification by column chromatography (cyclohexane/ethyl acetate = 2:1) the corresponding alcohol **1b-h** was obtained. Compound **1i** was used in the next reaction step without further purification.

*4.1.4. General procedure for the synthesis of cinnamyl azides (**2a-i**)*

Cinnamyl azides were prepared according to the literature procedure [34]. To a solution of cinnamyl alcohol **1a-i** (0.5 mmol) in dry THF, ADMP (0.171 g, 0.6 mmol) and DBU (0.099 g, 0.65 mmol) were added at 0 °C. The reaction was stirred for 10 min at 0 °C, diluted with saturated NH_4Cl solution and extracted with DCM (2 × 30 mL). Organic layers were collected and extracted with brine (2 × 30 mL), dried over anhydrous sodium sulfate and evaporated under reduced pressure. After purification by column chromatography (cyclohexane/ethyl acetate = 9:1) compounds **2a-i** were obtained.

*4.1.4.1. [(1E)-3-azidoprop-1-en-1-yl]benzene (**2a**).* From the reaction of 0.067 g cinnamyl alcohol, 0.171 g ADMP and 0.097 mL DBU and after purification by column chromatography (mobile phase cyclohexane/ethyl acetate = 9:1) 0.054 g (68%) of compound **2a** was obtained; oil; IR (film, ν/cm^{-1}) 3027, 2926, 2100, 1493, 1448, 1351, 1236, 967, 883, 746, 693; ^{1}H NMR (DMSO-d_6) δ 7.51–7.28 (m, 5H), 6.71 (d, 1H, J = 15.8 Hz), 6.44–6.34 (m, 1H), 4.04 (d, 2H, J = 6.5 Hz); ^{13}C NMR (DMSO-d_6) δ 136.31, 134.24, 129.16, 128.53, 127.00, 123.56, 52.60.

*4.1.4.2. 1-[(1E)-3-azidoprop-1-en-1-yl]-4-methoxybenzene (**2b**).* From the reaction of 0.082 g **1b**, 0.171 g ADMP and 0.097 mL DBU and after purification by column chromatography (mobile phase cyclohexane/ethyl acetate = 9:1) 0.039 g (41%) of compound **2b** was obtained; oil; IR (film, ν/cm^{-1}) 3035, 3004, 2953, 2935, 2837, 2101, 1652, 1607, 1512, 1464, 1250, 1175, 1034, 970, 841, 803; ^{1}H NMR (DMSO-d_6) δ 7.44–7.71 (m, 2H), 6.93–6.89 (m, 2H), 6.65 (d, 1H, J = 15.8 Hz), 6.27–6.18 (m, 1H), 3.99 (d, 2H, J = 6.7 Hz); ^{13}C NMR (DMSO-d_6) δ 159.23, 133.69, 128.44, 127.89, 120.42, 114.11, 55.13, 52.36.

*4.1.4.3. 5-[(1E)-3-azidoprop-1-en-1-yl]-2H-1,3-benzodioxole (**2c**).* From the reaction of 0.089 g **1c**, 0.171 g ADMP and 0.097 mL DBU and after purification by column chromatography (mobile phase cyclohexane/ethyl acetate = 9:1) 0.030 g (30%) of compound **2c** was obtained; oil; IR (film, ν/cm^{-1}) 2898, 2780, 2101, 1652, 1607, 1504, 1490, 1360, 1251, 1102, 1040, 966, 932, 862, 797; ^{1}H NMR (DMSO-d_6) δ 7.17 (d, 1H, J = 1.3 Hz), 6.96–6.83 (m, 1H), 6.62 (d, 1H, J = 15.8 Hz), 6.30–6.20 (m, 1H), 3.99 (dd, 1H, J = 6.6, 0.8 Hz); ^{13}C NMR (DMSO-d_6) δ 147.82, 147.24, 133.71, 130.28, 121.61, 121.04, 108.29, 105.62, 101.11, 52.25.

*4.1.4.4. 1-[(1E)-3-azidoprop-1-en-1-yl]-3-fluorobenzene (**2d**).* From the reaction of 0.076 g **1d**, 0.171 g ADMP and 0.097 mL DBU and after purification by column chromatography (mobile phase cyclohexane/ethyl acetate = 9:1) 0.077 g (87%) of compound **2d** was obtained; oil; IR (film, ν/cm^{-1}) 2958, 2928, 2870, 2102, 1611, 1584, 1490, 1446, 1350, 1269, 1250, 1146, 965, 871, 779, 682; ^{1}H NMR (DMSO-d_6) δ 7.45–7.29 (m, 3H), 7.18–7.04 (m, 1H), 6.71 (d, 1H, J = 15.9 Hz), 6.52–6.44 (m, 1H), 4.06 (dd, 2H, J = 6.4, 1.1 Hz); ^{13}C NMR (DMSO-d_6) δ 162.53 (d, J = 243.0 Hz), 138.54 (d, J = 8.0 Hz), 132.27, 130.61 (d, J = 8.5 Hz), 125.04, 122.94, 114.72 (d, J = 21.3 Hz), 112.78 (d, J = 22.0 Hz), 51.94.

*4.1.4.5. 1-[(1E)-3-azidoprop-1-en-1-yl]-4-fluorobenzene (**2e**).* From the reaction of 0.076 g **1e**, 0.171 g ADMP and 0.097 mL DBU and after purification by column chromatography (mobile phase cyclohexane/ethyl acetate = 9:1) 0.045 g (51%) of compound **2e** was obtained; oil; IR (film, ν/cm^{-1}) 3041, 2926, 2869, 2101, 1602, 1506, 1350, 1230, 968, 845, 804, 771; ^{1}H NMR (DMSO-d_6) δ 7.63–7.48 (m, 2H), 7.24–7.13 (m, 2H), 6.71 (d, 1H, J = 15.9 Hz), 6.39–6.32 (m, 1H), 4.03 (dd, 2H, J = 6.5, 0.9 Hz); ^{13}C NMR (DMSO-d_6) δ 161.87 (d, J = 245.0 Hz), 132.55, 132.44, 128.52 (d, J = 8.3 Hz), 123.03, 115.55 (d, J = 21.5 Hz), 52.09.

*4.1.4.6. 4-[(1E)-3-azidoprop-1-en-1-yl]-1,2-difluorobenzene (**2f**).* From the reaction of 0.085 g **1f**, 0.171 g ADMP and 0.097 mL DBU and after purification by column chromatography (mobile phase cyclohexane/ethyl acetate = 9:1) 0.059 g (60%) of compound **2f** was obtained; oil; IR (film, ν/cm^{-1}) 3038, 2928, 2070, 2102, 1604, 1516, 1434, 1294, 1275, 1212, 1147, 1115, 966, 872, 773; ^{1}H NMR (DMSO-d_6) δ 7.68–7.62 (m, 1H), 7.48–7.27 (m, 2H), 6.68 (d, 1H, J = 15.8 Hz), 6.47–6.40 (m, 1H), 4.05 (dd, 2H, J = 6.4, 1.0 Hz); ^{13}C NMR (DMSO-d_6) δ 150.95–147.49 (m, 6, 7), 133.85, 131.36, 124.87, 123.74, 117.67 (d, J = 17.2 Hz), 114.98 (d, 17.5 Hz), 51.90.

*4.1.4.7. 1-[(1E)-3-azidoprop-1-en-1-yl]-4-chlorobenzene (**2g**).* From the reaction of 0.084 g **1g**, 0.171 g ADMP and 0.097 mL DBU and after purification by column chromatography (mobile phase cyclohexane/ethyl acetate = 9:1) 0.070 g (72%) of compound **2g** was obtained; oil; IR (film, ν/cm^{-1}) 3034, 2927, 2855, 2100, 1594, 1492, 1255, 1091, 1013, 968, 844, 796; ^{1}H NMR (DMSO-d_6) δ 7.56–7.50 (m, 2H), 7.45–7.39 (m, 2H), 6.70 (d, 1H, J = 15.9 Hz), 6.46–6.39 (m, 1H), 4.05 (dd, 2H, J = 6.5, 1.2 Hz); ^{13}C NMR (DMSO-d_6) δ 134.84, 132.43, 132.27, 128.68, 128.27, 124.23, 52.02.

*4.1.4.8. 1-[(1E)-3-azidoprop-1-en-1-yl]-3-bromobenzene (**2h**).* From the reaction of 0.107 g **1h**, 0.171 g ADMP and 0.097 mL DBU and after purification by column chromatography (mobile phase cyclohexane/ethyl acetate = 9:1) 0,061 g (51%) of compound **2h** was obtained; oil; IR (film, ν/cm^{-1}) 3062, 3034, 2926, 2868, 2100, 1595, 1563, 1472, 1348, 1267, 1237, 1072, 996, 964, 878, 774, 679; ^{1}H NMR (DMSO-d_6) δ 7.72 (t, 1H, J = 1.8 Hz), 7.55–7.42 (m, 2H), 7.32 (t, 1H, J = 7.8 Hz), 6.68 (d, 1H, J = 15.9 Hz), 6.53–6.45 (m, 1H), 4.06 (dd, 2H, J = 6.4, 1.1 Hz); ^{13}C NMR (DMSO-d_6) δ 138.46, 131.90, 130.79, 130.65, 129.05, 125.58, 125.22, 122.18, 51.95.

*4.1.4.9. [(1E)-3-azido-2-methylprop-1-en-1-yl]benzene (**2i**).* From the reaction of 0.074 g **1i**, 0.171 g ADMP and 0.097 mL DBU and after purification by column chromatography (mobile phase cyclohexane/ethyl acetate = 9:1) 0,061 g (71%) of compound **2i** was obtained; oil; IR (film, ν/cm^{-1}) 3035, 2926, 2068, 2101, 1605, 1510, 1351, 1290, 1115, 968, 883, 746, 693 cm^{-1}; ^{1}H NMR (DMSO-d_6) δ 7.41–7.27 (m, 5H), 6.57 (s, 1H), 4.00 (s, 3H), 1.89 (s, 3H); ^{13}C NMR (DMSO-d_6) δ 136.50, 132.75, 128.75, 128.33, 128.25, 126.90, 58.67, 16.15.

*4.1.5. 7-Methoxy-1-methyl-9-(prop-2-yn-1-yl)-9H-pyrido[3,4-b] indole (**3**)*

Harmine (0.212 g, 1 mmol) was dissolved in dry DMF (4 mL). Under argon atmosphere 60% dispersion of sodium hydride in mineral oil (0.108 g, 2.7 mmol) was added, followed by a dropwise addition of 80% solution of propargyl bromide in toluene (0.284 mL, 3 mmol). The reaction was stirred at r.t. and under argon atmosphere for 2 h. Upon completion, reaction mixture was poured in 50 mL water. Product was extracted with DCM (4 × 30 mL). Organic layers were collected and washed with water, dried over anhydrous sodium sulfate and evaporated under reduced pressure. After purification by column chromatography (DCM/methanol = 9.5:0.5) and trituration with diethyl ether 0.138 g (55%) of **3** was obtained; mp 147–149 °C; IR (KBr, ν/cm^{-1}) 3270, 3064, 2118, 1616, 1568, 1494, 1450, 1402, 1340, 1294, 1254, 1226, 1192, 1170, 1138, 1042, 976, 1042, 976, 922, 830, 806, 722, 690, 648; ^{1}H NMR (DMSO-d_6) δ 8.20 (d, 1H, J = 5.2 Hz), 8.10 (d, 1H, J = 8.6 Hz), 7.88 (d, 1H, J = 5.2 Hz), 7.33 (d, 1H, J = 2.1 Hz), 6.90 (dd, 1H, J = 8.6 Hz, 2.1 Hz), 5.45 (d, 2H, J = 2.3 Hz), 3.91 (s, 3H), 3.37 (t, 1H, J = 2.3 Hz), 3.05 (s, 3H); ^{13}C NMR (DMSO-d_6) δ 160.72, 142.60, 141.09, 138.53, 134.40, 128.92, 122.50, 114.42, 112.29, 109.70, 93.83, 80.25, 75.59, 55.68, 34.22, 22.49.

*4.1.6. 1-Methyl-7-(prop-2-yn-1-yloxy)-9H-pyrido[3,4-b]indole (**4**)*

Harmole (0.198 g, 1 mmol) was dissolved in dry DMF (4 mL). Under argon atmosphere cesium carbonate (0.456 g, 1.4 mmol) was added, followed by dropwise addition of 80% solution of propargyl bromide in toluene (0.095 mL, 1.1 mmol). The reaction was stirred at r.t. and under argon atmosphere for 2 h. Upon completion, reaction mixture was poured in 50 mL water. Product was extracted with DCM (4 × 30 mL). Organic layers were collected and washed with water, dried over anhydrous sodium sulfate and evaporated under reduced pressure. After purification by column chromatography (DCM/methanol = 9.7:0.3, 9.5:0.5) and trituration with diethyl ether 0.132 g (56%) of **4** was obtained; mp 159–161 °C; IR (KBr, ν/cm^{-1}) 3272, 3068, 2960, 2868, 2774, 2118, 1632, 1566, 1484, 1454, 1328, 1276, 1166, 1136, 1108, 1070, 1024, 948, 816, 704, 684; ^{1}H NMR (DMSO-d_6) δ 11.55 (s, 1H), 8.17 (d, 1H, J = 5.3 Hz), 8.10 (d, 1H, J = 8.7 Hz), 7.85 (d, 1H, J = 5.3 Hz), 7.13 (d, 1H, J = 2.1 Hz), 6.89 (dd, 1H, J = 8.7 Hz, 2.3 Hz), 4.93 (d, 2H, J = 2.3 Hz), 3.64 (t, 1H, J = 2.3 Hz), 2.74 (s, 3H); ^{13}C NMR (DMSO-d_6) δ 157.94, 141.67, 141.33, 137.59, 134.60, 127.17, 122.68, 115.35, 112.06, 109.55, 96.00, 78.44, 55.75, 20.22.

*4.1.7. 1-Methyl-9-(prop-2-yn-1-yl)-7-(prop-2-yn-1-yloxy)-9H-pyrido[3,4-b]indole (**5**)*

Harmole (0.198 g, 1 mmol) was dissolved in dry DMF (4 mL). Under argon atmosphere cesium carbonate (0.912 g, 2.8 mmol) was added, followed by dropwise addition of 80% solution of propargyl bromide in toluene (0.190 mL, 2.2 mmol). The reaction was stirred at r.t. and under argon atmosphere for 2 h. Upon completion, reaction mixture was poured in 50 mL water. Product was extracted with DCM (4 × 30 mL). Organic layers were collected and washed with water, dried over anhydrous sodium sulfate and evaporated under reduced pressure. After purification by column chromatography (DCM/methanol = 9.7:0.3, 9.5:0.5) and trituration with ether 0.164 g (60%) of **5** was obtained; mp 147–149 °C; IR (KBr, ν/cm^{-1}) 3288, 3178, 2926, 2108, 1626, 1566, 1500, 1444, 1404, 1372, 1330, 1260, 1182, 1140, 1042, 176, 928, 814, 718, 686; ^{1}H NMR (DMSO-d_6) δ 8.22 (d, 1H, J = 5.2 Hz), 8.14 (d, 1H, J = 8.6 Hz), 7.91 (d, 1H, J = 5.2 Hz), 7.41 (d, 1H, J = 2.0 Hz), 6.97 (dd, 1H, J = 8.6 Hz, 2.1 Hz), 5.43 (d, 2H, J = 2.2 Hz), 4.97 (d, 2H, J = 2.3 Hz), 3.61 (t, 1H, J = 2.3 Hz), 3.37 (t, 1H, J = 2.2 Hz), 3.06 (s, 3H); ^{13}C NMR (DMSO-d_6) δ 158.50, 142.34, 141.20, 138.59, 134.51, 128.81, 122.55, 115.08, 112.41, 109.78, 95.44, 80.14, 79.19, 78.32, 75.64, 56.00, 39.73, 34.27, 22.49.

*4.1.8. General procedure for the synthesis of N-harmicines **6a-i***

N-harmicines were prepared according to the literature procedure [35]. In short, to a solution of compound **3** (0.05 g, 0.2 mmol) and the corresponding cinnamyl azide **2a-i** (0.22 mmol) in methanol (6 mL) $Cu(OAc)_2$ (0.01 mmol) was added. The reaction mixture was stirred overnight at r.t. The solvent was removed under reduced pressure.

*4.1.8.1. 4-({7-Methoxy-1-methyl-9H-pyrido[3,4-b]indol-9-yl} methyl)-1-[(2E)-3-phenylprop-2-en-1-yl]-1H-1,2,3-triazole (**6a**).* From the reaction of 0.035 g **2a** and 0.05 g **3** and after purification by column chromatography (mobile phase dichloromethane/methanol 9.7:0.3 and 9.5:0.5) and trituration with diethyl ether 0.052 g (64%) of **6a** was obtained; mp 202–203 °C; IR (KBr, ν/cm^{-1}) 3122, 3079, 2935, 1621, 1570, 1496, 1450, 1404, 1343, 1253, 1218, 1177, 1129, 1096, 1049, 973, 924, 848, 817, 771, 740, 697; ^{1}H NMR (DMSO-d_6) δ 8.19 (d, 1H, J = 5.2 Hz), 8.11 (d, 1H, J = 8.6 Hz), 8.02 (s, 1H), 7.91 (d, 1H, J = 5.2 Hz), 7.40–7.23 (m, 6H), 6.89 (dd, 1H, J = 8.6, 2.1 Hz), 6.54–6.40 (m, 2H), 5.90 (s, 2H), 5.09 (d, 2H, J = 5.4 Hz), 3.88 (s, 3H), 3.06 (s, 3H); ^{13}C NMR (DMSO-d_6) δ 160.69, 144.06, 142.84, 140.96, 137.66, 135.65, 134.60, 133.35, 128.77, 128.67, 128.11, 126.49, 123.75, 122.91, 122.50, 114.42, 112.37, 109.50, 94.12, 55.65, 51.25, 39.73, 22.97; ESI-MS: *m/z* 410.1 $(M+1)^+$; Anal. Calcd. for $C_{25}H_{23}N_5O$: C, 73.33; H, 5.66; N, 17.10, found: C, 73.38; H, 5.41; N, 17.39.

*4.1.8.2. 4-({7-Methoxy-1-methyl-9H-pyrido[3,4-b]indol-9-yl} methyl)-1-[(2E)-3-(4-methoxy phenyl)prop-2-en-1-yl]-1H-1,2,3-triazole (**6b**).* From the reaction of 0.042 g **2b** and 0.05 g **3** and after purification by column chromatography (mobile phase cyclohexane/ethyl acetate/methanol 3:1:0.5) and trituration with diethyl ether 0.062 g (71%) of **6b** was obtained; mp 178–179 °C; IR (KBr, ν/cm^{-1}) 3127, 3083, 2956, 2837, 1622, 1567, 1511, 1445, 1406, 1343, 1251, 1176, 1135, 1051, 974, 926, 825; ^{1}H NMR (DMSO-d_6) δ 8.17 (d, 1H, J = 5.2 Hz), 8.09 (d, 1H, J = 8.6 Hz), 7.99 (s, 1H), 7.87 (d, 1H, J = 5.2 Hz), 7.34–7.31 (m, 3H), 6.90–6.86 (m, 3H), 6.47 (d, 1H, J = 15.8 Hz), 6.30–6.23 (m, 1H), 5.88 (s, 2H), 5.05 (d, 2H, J = 6.0 Hz), 3.88 (s, 3H), 3.74 (s, 3H), 3.05 (s, 3H); ^{13}C NMR (DMSO-d_6) δ160.56, 159.21, 144.09, 142.68, 141.14, 138.08, 134.67, 133.14, 128.77, 134.60, 128.53, 122.78, 122.40, 121.15, 114.48, 114.07, 112.27, 109.34, 94.13, 55.62, 55.12, 51.3, 39.73, 23.24; ESI-MS: *m/z* 440.2 $(M+1)^+$; Anal. Calcd. for $C_{26}H_{25}N_5O_2$: C, 71.05; H, 5.73; N, 15.93, found: C, 71.13; H, 5.62; N, 15.65.

*4.1.8.3. 1-[(2E)-3-(2H-1,3-benzodioxol-5-yl)prop-2-en-1-yl]-4-({7-methoxy-1-methyl-9H-pyrido[3,4-b]indol-9-yl}methyl)-1H-1,2,3-triazole (**6c**).* From the reaction of 0.045 g **2c** and 0.05 g **3** and after purification by column chromatography (mobile phase cyclohexane/ethyl acetate/methanol 3:1:0.5) and trituration with diethyl ether 0.056 g (62%) of **6c** was obtained; mp 203–204 °C; IR (KBr, ν/cm^{-1}) 3427, 3123, 3057, 2996, 2930, 1622, 1570, 1497, 1448, 1405, 1351, 1300, 1250, 1167, 1127, 1038, 970, 926, 815, 726; ^{1}H NMR (DMSO-d_6) δ 8.18 (d, 1H, J = 5.2 Hz), 8.10 (d, 1H, J = 8.6 Hz), 7.99 (s, 1H), 7.89 (d, 1H, J = 5.2 Hz), 7.34 (d, 1H, J = 2.0 Hz), 7.07 (d, 1H,

J = 1.4 Hz), 6.91–6.78 (m, 3H), 6.44 (d, 1H, J = 15.8 Hz), 6.33–6.24 (m, 1H), 6.00 (s, 2H), 5.88 (s, 2H), 5.04 (d, 2H, J = 6.2 Hz), 3.88 (s, 3H), 3.05 (s, 3H); ^{13}C NMR (DMSO-d_6) δ 160.61, 147.48, 147.23, 144.04, 142.75, 141.02, 137.82, 134.62, 133.25, 130.09, 128.64, 122.77, 122.43, 121.69, 121.57, 114.43, 112.30, 109.39, 108.24, 105.54, 101.10, 94.13, 69.77, 55.62, 51.28, 39.71, 23.07; ESI-MS: m/z 454.1 $(M+1)^+$; Anal. Calcd. for $C_{26}H_{23}N_5O_3$: C, 68.86; H, 5.11; N, 15.44, found: C, 68.72; H, 5.37; N, 15.21.

*4.1.8.4. 1-[(2E)-3-(3-fluorophenyl)prop-2-en-1-yl]-4-({7-methoxy-1-methyl-9H-pyrido[3,4-b]indol-9-yl}methyl)-1H-1,2,3-triazole (**6d**).* From the reaction of 0.039 g **2d** and 0.05 g **3** and after purification by column chromatography (mobile phase cyclohexane/ethyl acetate/methanol 3:1:0.5) and trituration with diethyl ether 0.053 g (62%) of **6d** was obtained; mp 179–180 °C; IR (KBr, ν/cm^{-1}) 3124, 3078, 2947, 2841, 1621, 1583, 1563, 1496, 1442, 1406, 1383, 1359, 1343, 1253, 1222, 1196, 1174, 1139, 1095, 1045, 976, 925, 812, 786; ^{1}H NMR (DMSO-d_6) δ 8.18 (d, 1H, J = 5.2 Hz), 8.09 (d, 1H, J = 8.6 Hz), 8.01 (s, 1H), 7.88 (d, 1H, J = 5.2 Hz), 7.37–7.07 (m, 5H), 6.89 (dd, 1H, J = 8.6,2.2 Hz), 6.56–6.46 (m, 2H), 5.89 (s, 2H), 5.10 (d, 2H, J = 5.0 Hz), 3.88 (s, 3H), 3.05 (s, 3H); ^{13}C NMR (DMSO-d_6) δ 162.48 (d, J = 244.4 Hz), 160.56, 144.14, 142.68, 141.15, 138.31 (d, J = 8.0 Hz), 138.09, 134.67, 132.05, 1130,60 (d, J = 8.6 Hz), 128.55, 125.58, 122.96, 122.94, 122.41, 114.80 (d, J = 21.5 Hz), 114.50, 112.74 (d, J = 21.5 Hz), 112.28, 109.34, 94.14, 55.62, 51.09, 39.73, 23.24; ESI-MS: m/z 428.2 $(M+1)^+$; Anal. Calcd. for $C_{25}H_{22}FN_5O$: C, 70.24; H, 5.19; N, 16.38, found: C, 70.33; H, 5.13; N, 16.14.

*4.1.8.5. 1-[(2E)-3-(4-fluorophenyl)prop-2-en-1-yl]-4-({7-methoxy-1-methyl-9H-pyrido[3,4-b]indol-9-yl}methyl)-1H-1,2,3-triazole (**6e**).* From the reaction of 0.039 g **2e** and 0.05 g **3** and after purification by column chromatography (mobile phase cyclohexane/ethyl acetate/methanol 3:1:0.5) and trituration with diethyl ether 0.048 g (56%) of **6e** was obtained; mp 188–190 °C; IR (KBr, ν/cm^{-1}) 3126, 3048, 3000, 2930, 2836, 1626, 1562, 1510, 1450, 1408, 1324, 1252, 1224, 1168, 1136, 1044, 970, 924, 846, 816, 738; ^{1}H NMR (DMSO-d_6) δ 8.18 (d, 1H, J = 5.2 Hz), 8.09 (d, 1H, J = 8.6 Hz), 8.00 (s, 1H), 7.88 (d, 1H, J = 5.2 Hz), 7.49–7.40 (m, 2H), 7.34 (d, 1H, J = 2.1 Hz), 7.20–7.10 (m, 2H), 6.88 (dd, 1H, J = 8.6, 2.2 Hz), 6.51 (d, 1H, J = 15.9 Hz), 6.43–6.36 (m, 1H), 5.89 (s, 2H), 5.08 (d, 2H, J = 6.0 Hz), 3.88 (s, 3H), 3.05 (s, 3H); ^{13}C NMR (DMSO- d_6) δ 161.86 (d, J = 245.3 Hz), 160.55 (1), 144.11 (2′), 142.67 (8), 141.12 (11), 138.06 (3), 134.65 (9), 132.26 (7′), 132.20 (5′), 128.52 (4), 128.48 (d, 8′, 12′, J = 8.0 Hz), 123.65 (3′), 122.85 (6′), 122.38 (3), 115.52 (d, 9′, 11′, J = 21.5 Hz), 114.48 (5), 112.25 (6), 109.32 (2), 94.13 (12), 55.61 (14), 51.20 (4′), 39.73 (1′), 23.22 (13); ESI-MS: m/z 428.2 $(M+1)^+$; Anal. Calcd. for $C_{25}H_{22}FN_5O$: C, 70.24; H, 5.19; N, 16.38, found: C, 70.39; H, 5.28; N, 16.10.

*4.1.8.6. 1-[(2E)-3-(3,4-difluorophenyl)prop-2-en-1-yl]-4-({7-methoxy-1-methyl-9H-pyrido[3,4-b]indol-9-yl}methyl)-1H-1,2,3-triazole (**6f**).* From the reaction of 0.043 g **2f** and 0.05 g **3** and after purification by column chromatography (mobile phase cyclohexane/ethyl acetate/methanol 3:1:0.5) and trituration with diethyl ether 0.049 g (55%) of **6f** was obtained; mp 166–167 °C; IR (KBr, ν/cm^{-1}) 3120, 3068, 3006, 2964, 2840, 1626, 1568, 1518, 1452, 1410, 1348, 1296, 1252, 1228, 1168, 1138, 1116, 1048, 1026, 974, 926, 888, 818, 738; ^{1}H NMR (DMSO-d_6) δ 8.18 (d, 1H, J = 5.2 Hz), 8.09 (d, 1H, J = 8.6 Hz), 8.00 (s, 1H), 7.88 (d, 1H, J = 5.2 Hz), 7.57–7.52 (m, 1H), 7.41–7.33 (m, 1H), 7.34 (d, 1H, J = 2.1 Hz), 7.24–7.20 (m, 1H), 6.89 (dd, 1H, J = 8.6,2.1 Hz), 6.49–6.48 (m, 2H), 5.89 (s, 2H), 5.09 (d, 2H, J = 2.3 Hz), 3.88 (s, 3H), 3.05 (s, 3H); ^{13}C NMR (DMSO-d_6) δ 160.55, 150.57 (dd, J = 53.1, 12.2 Hz), 148.13 (dd, J = 55.1, 12.3 Hz), 144.12, 142.66, 141.13, 138.08, 134.65, 133.62, 131.23, 128.53, 125.37, 123.75 (d, J = 3.2 Hz), 122.91, 122.39, 117.64 (d, J = 17.2 Hz), 114.94 (d, J = 17.6 Hz), 114.48, 112.26, 109.31, 94.14, 55.60, 51.04, 39.93, 23.23; ESI-MS: m/z 446.2 $(M+1)^+$; Anal. Calcd. for $C_{25}H_{21}F_2N_5O$: C, 67.41; H, 4.75; N, 15.72, found: C, 67.30; H, 4.63; N, 15.96.

*4.1.8.7. 1-[(2E)-3-(4-chlorophenyl)prop-2-en-1-yl]-4-({7-methoxy-1-methyl-9H-pyrido[3,4-b]indol-9-yl}methyl)-1H-1,2,3-triazole (**6g**).* From the reaction of 0.043 g **2g** and 0.05 g **3** and after purification by column chromatography (mobile phase cyclohexane/ethyl acetate/methanol 3:1:0.5) and trituration with diethyl ether 0.050 g (56%) of **6g** was obtained; mp 177–178 °C; IR (KBr, ν/cm^{-1}) 3126, 3048, 3000, 2930, 2836, 1626, 1562, 1510, 1450, 1408, 1324, 1252, 1224, 1168, 1136, 1044, 970, 924, 846, 816, 738; ^{1}H NMR (DMSO-d_6) δ 8.18 (d, 1H, J = 5.2 Hz), 8.09 (d, 1H, J = 8.6 Hz), 8.00 (s, 1H), 7.87 (d, 1H, J = 5.2 Hz), 7.43–7.36 (m, 4H), 7.34 (d, 1H, J = 2.1 Hz), 6.89 (dd, 1H, J = 8.6, 2.2 Hz), 6.52–6.46 (m, 2H), 5.89 (s, 2H), 5.09 (d, 2H, J = 4.8 Hz), 3.88 (s, 3H), 3.04 (s, 3H); ^{13}C NMR (DMSO-d_6) δ 160.54, 144.12, 142.66, 141.12, 138.08, 134.65, 134.62, 132.47, 131.98, 128.64, 128.22, 128.53, 124.80, 122.90, 122.38, 114.48, 112.25, 109.31, 94.13, 55.61, 51.15, 39.73, 23.23; ESI-MS: m/z 444.2 $(M+1)^+$; Anal. Calcd. for $C_{25}H_{22}ClN_5O$: C, 67.64; H, 5.00; N, 15.78, found: C, 67.69; H, 5.22; N, 15.71.

*4.1.8.8. 1-[(2E)-3-(3-bromophenyl)prop-2-en-1-yl]-4-({7-methoxy-1-methyl-9H-pyrido[3,4-b]indol-9-yl}methyl)-1H-1,2,3-triazole (**6h**).* From the reaction of 0.052 g **2h** and 0.05 g **3** and after purification by column chromatography (mobile phase cyclohexane/ethyl acetate/methanol 3:1:0.5) and trituration with diethyl ether 0.071 g (72%) of **6h** was obtained; mp 183–184 °C; IR (KBr, ν/cm^{-1}) 3130, 3048, 2924, 2834, 1624, 1562, 1500, 1450, 1410, 1324, 1306, 1254, 1226, 1254, 1226, 1172, 1138, 1042, 970, 924, 876, 818, 742; ^{1}H NMR (DMSO-d_6) δ 8.18 (d, 1H, J = 5.2 Hz), 8.09 (d, J = 8.6 Hz, 1H), 8.01 (s, 1H), 7.88 (d, 1H, J = 5.2 Hz), 7.61 (s, 1H), 7.45 (d, 1H, J = 7.9 Hz), 7.39 (d, 1H, J = 7.8 Hz), 7.35 (d, 1H, J = 2.0 Hz), 7.28 (t, 1H, J = 7.8 Hz), 6.89 (dd, 1H, J = 8.6, 2.1 Hz), 6.58–6.51 (m, 1H), 6.46 (d, 1H, J = 16.0 Hz), 5.89 (s, 2H), 5.10 (d, 2H, J = 5.8 Hz), 3.88 (s, 3H), 3.05 (s, 3H); ^{13}C NMR (DMSO-d_6) δ 160.54, 144.11, 142.66, 141.13, 138.22, 138.08, 134.66, 131.64, 130.75, 130.69, 128.99, 128.52, 125.75, 125.53, 122.94, 122.38, 122.13, 114.48, 112.25, 109.33, 94.13, 55.61, 51.08, 39.73, 23.24; ESI-MS: m/z 488.1 $(M+1)^+$, 490.1 $(M+2+1)^+$; Anal. Calcd. for $C_{25}H_{22}BrN_5O$: C, 61.48; H, 4.54; N, 14.34, found: C, 61.31; H, 4.59; N, 14.10.

*4.1.8.9. 4-({7-Methoxy-1-methyl-9H-pyrido[3,4-b]indol-9-yl}methyl)-1-[(2E)-2-methyl-3-phenylprop-2-en-1-yl]-1H-1,2,3-triazole (**6i**).* From the reaction of 0.038 g **2i** and 0.05 g **3** and after purification by column chromatography (mobile phase cyclohexane/ethyl acetate/methanol 1:1:0.5) and trituration with diethyl ether 0.053 g (63%) of **6i** was obtained; mp 151–152 °C; IR (KBr, ν/cm^{-1}) 3427, 3129, 3057, 2993, 2932, 2839, 1625, 1570, 1496, 1450, 1406, 1340, 1298, 1250, 1219, 1172, 1127, 1042, 973, 924, 815, 743, 700; ^{1}H NMR (DMSO-d_6) δ 8.18 (d, 1H, J = 5.1 Hz), 8.09 (d, 1H, J = 8.6 Hz), 7.99 (s, 1H), 7.88 (d, 1H, J = 5.2 Hz), 7.36–7.24 (m, 5H), 7.18 (d, 1H, J = 7.6 Hz), 6.88 (dd, 1H, J = 8.6, 1.8 Hz), 6.29 (s, 1H), 5.90 (s, 2H), 5.02 (s, 2H), 3.88 (s, 3H), 3.04 (s, 3H), 1.68 (s, 3H); ^{13}C NMR (DMSO-d_6) δ 160.54, 144.06, 142.71, 141.06, 138.01, 136.25, 134.66, 132.87, 128.58, 128.24, 127.91, 126.88, 123.22, 122.32, 114.47, 112.18, 109.32, 94.09, 57.01, 55.58, 39.75, 23.10, 15.44; ESI-MS: m/z 424.2 $(M+1)^+$; Anal. Calcd. for $C_{26}H_{25}N_5O$: C, 73.74; H, 5.95; N, 16.54, found: C, 73.39; H, 5.76; N, 16.68.

*4.1.9. General procedure for the synthesis of O-harmicines **7a-i***

O-harmicines were prepared according to the literature procedure [35]. In short, propargyl derivative **4** (0.047 g, 0.2 mmol) and the corresponding cinnamyl azide **2a-i** (0.22 mmol) were dissolved in methanol (6 mL) and $Cu(OAc)_2$ (0.01 mmol) was added. The reaction mixture was stirred overnight at r. t. The solvent was

removed under the reduced pressure.

*4.1.9.1. 4-[({1-Methyl-9H-pyrido[3,4-b]indol-7-yl}oxy)methyl]-1-[(2E)-3-phenylprop-2-en-1-yl]-1H-1,2,3-triazole (**7a**).* From the reaction of 0.035 g **2a** and 0.047 g **4** and after purification by column chromatography (mobile phase DCM/methanol 9.5:0.5) 0.029 g (37%) of **7a** was obtained; mp 133–134 °C; IR (KBr, ν/cm^{-1}) 1630, 1560, 1450, 1422, 1328, 1278, 1216, 1172, 1052, 1008, 968, 804, 772, 692, 650; ^{1}H NMR (DMSO-d_6) δ 11.47 (s, 1H), 8.30 (s, 1H), 8.15 (d, 1H, J = 4.4 Hz), 8.06 (d, 1H, J = 8.7 Hz), 7.80 (d, 1H, J = 5.1 Hz), 7.44–7.26 (m, 5H), 7.18 (d, 1H, J = 2.0 Hz), 6.90 (dd, 1H, J = 8.7,2.1 Hz), 6.64–6.47 (m, 2H), 5.29 (s, 1H), 5.21 (d, 2H, J = 5.7 Hz), 2.72 (s, 3H); ^{13}C NMR (DMSO-d_6) δ 158.72, 143.00, 141.76, 141.32, 137.72, 135.68, 133.58, 128.61, 128.08, 127.11, 126.51, 124.42, 123.64, 122.56, 115.13, 111.89, 109.46, 95.93, 61.51, 51.30, 20.27; ESI-MS: *m/z* 396.3 (M+1)$^+$; Anal. Calcd. for $C_{24}H_{21}N_5O$: C, 72.89; H, 5.35; N, 17.71, found: C, 73.09; H, 5.61; N, 17.52.

*4.1.9.2. 1-[(2E)-3-(4-methoxyphenyl)prop-2-en-1-yl]-4-[({1-methyl-9H-pyrido[3,4-b]indol-7-yl}oxy)methyl]-1H-1,2,3-triazole (**7b**).* From the reaction of 0.042 g **2b** and 0.047 g **4** and after purification by column chromatography (mobile phase DCM/methanol 9.5:0.5) and trituration with diethyl ether/petrolether 0.049 g (57%) of **7b** was obtained; mp 215–216 °C; IR (KBr, ν/cm^{-1}) 3137, 3078, 2961, 2932, 2872, 2840, 1620, 1567, 1510, 1438, 1315, 1281, 1243, 1172, 1142, 1112, 1027, 969, 879, 815, 772, 741, 682, 634; ^{1}H NMR (DMSO-d_6) δ 11.65 (s, 1H), 8.29 (s, 1H), 8.19 (bs, 1H, J = 4.4 Hz), 8.10 (d, 1H, J = 8.7 Hz), 7.89 (d, 1H, J = 5.0 Hz), 7.35 (d, 2H, J = 8.7 Hz), 7.21 (d, 1H, J = 1.9 Hz), 6.93 (dd, 1H, J = 8.7,2.1 Hz), 6.86 (d, 2H, J = 8.7 Hz), 6.56 (d, 1H, J = 15.8 Hz), 6.41–6.31 (m, 1H), 5.31 (s, 2H), 5.17 (d, 2H, J = 6.3 Hz), 3.74 (s, 3H), 2.76 (s, 3H); ^{13}C NMR (DMSO-d_6) δ 159.21, 159.07 (1,10′), 142.90 (2′), 142.21 (8), 140.82 (11), 136.55 (7), 133.97 (9), 133.33 (5′), 128.28 (4), 127.88 (8′,12′), 127.77 (7′), 124.44 (3′), 122.89 (3), 121.07 (6′), 114.95 (5), 114.04 (9′,11′), 112.28 (6), 109.92 (2), 95.83 (12), 61.49 (1′), 55.10 (13′), 51.47 (4′), 19.73; ESI-MS: *m/z* 426.1 (M+1)$^+$; Anal. Calcd. for $C_{25}H_{23}N_5O_2$: C, 70.57; H, 5.45; N, 16.46, found: C, 70.85; H, 5.69; N, 16.74.

*4.1.9.3. 1-[(2E)-3-(2H-1,3-benzodioxol-5-yl)prop-2-en-1-yl]-4-[({1-methyl-9H-pyrido[3,4-b]indol-7-yl}oxy)methyl]-1H-1,2,3-triazole (**7c**).* From the reaction of 0.045 g **2c** and 0.047 g **4** and after purification by column chromatography (mobile phase cyclohexane/ethyl acetate/methanol 3:1:0.75) and trituration with diethyl ether/DCM 0.049 g (66%) of **7c** was obtained; mp 203–204 °C; IR (KBr, ν/cm^{-1}); 3180, 3103, 2883, 2779, 1626, 1569, 1496, 1447, 1385, 1331, 1258, 1173, 1138, 1107, 1038, 1006, 968, 927, 816; ^{1}H NMR (DMSO-d_6) δ 11.51 (s, 1H), 8.28 (s, 1H), 8.16 (d, 1H, J = 5.1 Hz), 8.07 (d, 1H, J = 8.7 Hz), 7.83 (d, 1H, J = 5.3 Hz), 7.19 (d, 1H, J = 2.0 Hz), 7.15 (s, 1H), 6.91 (dd, 1H, J = 8.7,2.2 Hz), 6.83 (s, 2H), 6.56 (d, 1H, J = 15.8 Hz), 6.43–6.33 (m, 1H), 6.01 (s, 2H), 5.29 (s, 1H), 5.16 (d, 2H, J = 6.2 Hz), 2.73 (s, 3H); ^{13}C NMR (DMSO-d_6) δ 158.86, 147.82, 147.28, 142.96, 141.91, 141.19, 137.39, 134.56, 133.56, 130.15, 127.33, 124.43, 122.72, 121.70, 121.62, 115.07, 112.05, 109.61, 108.24, 105.59, 101.12, 95.82, 61.47, 51.42, 20.14; ESI-MS: *m/z* 440.1 (M+1)$^+$; Anal. Calcd. for $C_{25}H_{21}N_5O_3$: C, 68.33; H, 4.82; N, 15.94, found: C, 68.49; H, 5.15; N, 15.69.

*4.1.9.4. 1-[(2E)-3-(3-fluorophenyl)prop-2-en-1-yl]-4-[({1-methyl-9H-pyrido[3,4-b]indol-7-yl}oxy)methyl]-1H-1,2,3-triazole (**7d**).* From the reaction of 0.039 g **2d** and 0.047 g **4** and after purification by column chromatography (mobile phase cyclohexane/ethyl acetate/methanol 3:1:0.75) and trituration with diethyl ether/DCM mixture 0.055 g (66%) of **7d** was obtained; mp 182–185 °C; IR (KBr, ν/cm^{-1}) 3187, 3133, 3104, 2877, 1628, 1583, 1569, 1487, 1448, 1387, 1327, 1297, 1276, 1239, 1175, 1141, 1108, 1056, 1033, 1011, 967, 869, 819, 788, 684; ^{1}H NMR (DMSO-d_6) δ 11.52 (s, 1H), 8.30 (s, 1H), 8.16 (d, 1H, J = 5.3 Hz), 8.06 (d, 1H, J = 8.7 Hz), 7.81 (d, 1H, J = 5.3 Hz), 7.37–7.32 (m, 5H), 6.91 (dd, 1H, J = 8.7,2.2 Hz), 6.63–6.62 (m, 2H), 5.30 (s, 2H), 5.23–5.22 (m, 2H), 2.72 (s, 3H); ^{13}C NMR (DMSO-d_6) δ 162.50 (d, J = 243.2 Hz), 158.74, 143.01, 141.80, 141.37, 138.36 (d, J = 7.9 Hz), 137.73, 134.60, 132.35, 130.58 (d, J = 8.5 Hz), 127.13, 125.49, 124.61, 123.03, 122.65, 115.11, 114.82 (d, J = 21.3 Hz), 112.78 (d, J = 21.9 Hz), 111.96, 109.48, 95.85, 61.46, 51.20, 20.34; ESI-MS: *m/z* 414.2 (M+1)$^+$; Anal. Calcd. for $C_{24}H_{20}FN_5O$: C, 69.72; H, 4.88; N, 16.94, found: C, 69.54; H, 4.97; N, 17.15.

*4.1.9.5. 1-[(2E)-3-(4-fluorophenyl)prop-2-en-1-yl]-4-[({1-methyl-9H-pyrido[3,4-b]indol-7-yl}oxy)methyl]-1H-1,2,3-triazole (**7e**).* From the reaction of 0.039 g **2e** and 0.047 g **4** and after purification by column chromatography (mobile phase cyclohexane/ethyl acetate/methanol 1:1:0.5) and trituration with diethyl ether 0.049 g (60%) of **7e** was obtained; mp 196–197 °C; IR (KBr, ν/cm^{-1}) 3370, 3147, 3094, 2947, 2900, 2870, 1632, 1602, 1569, 1511, 1482, 1450, 1419, 1367, 1322, 1276, 1235, 1179, 1135, 1107, 1072, 1048, 1028, 1013, 975, 943, 827, 801, 772, 739; ^{1}H NMR (DMSO-d_6) δ 11.47 (s, 1H), 8.29 (s, 1H), 8.16 (d, 1H, J = 5.3 Hz), 8.06 (d, 1H, J = 8.7 Hz), 7.81 (d, 1H, J = 5.3 Hz), 7.50–7.46 (m, 2H), 7.19 (d, 1H, J = 2.2 Hz), 7.17–7.10 (m, 2H), 6.91 (dd, 1H, J = 8.7,2.2 Hz), 6.62 (d, 1H, J = 15.9 Hz), 6.52–6.45 (m, 1H), 5.30 (s, 2H), 5.20 (d, 2H, J = 6.1 Hz), 2.72 (s, 13); ^{13}C NMR (DMSO-d_6) δ 161.90 (d, J = 245.2 Hz), 158.75, 143.02, 141.78, 141.36, 137.76, 134.60, 132.47, 132.29, 128.57 (d, J = 8.2 Hz), 127.15, 124.53, 123.59, 122.66, 115.53 (d, J = 21.5 Hz), 115.13, 111.98, 109.51, 95.86, 61.47, 51.33, 20.32; ESI-MS: *m/z* 414.2 (M+1)$^+$; Anal. Calcd. for $C_{24}H_{20}FN_5O$: C, 69.72; H, 4.88; F, 4.60; N, 16.94, found: C, 69.39; H, 4.84; N, 17.11.

*4.1.9.6. 1-[(2E)-3-(3,4-difluorophenyl)prop-2-en-1-yl]-4-[({1-methyl-9H-pyrido[3,4-b]indol-7-yl}oxy)methyl]-1H-1,2,3-triazole (**7f**).* From the reaction of 0.043 g **2f** and 0.047 g **4** and after purification by column chromatography (mobile phase cyclohexane/ethyl acetate/methanol 3:1:0.5) and trituration with diethyl ether 0.059 g (68%) of **7f** was obtained; mp 172–173 °C; IR (KBr, ν/cm^{-1}) 3400, 3274, 3052, 3014, 2934, 2876, 1630, 1568, 1514, 1432, 1272, 1238, 1172, 1110, 1056, 1010, 962, 868, 816, 634; ^{1}H NMR (DMSO-d_6) δ 11.47 (s, 1H), 8.30 (s, 1H), 8.15 (d, 1H, J = 5.3 Hz), 8.06 (d, 1H, J = 8.6 Hz), 7.81 (d, 1H, J = 5.3 Hz), 7.64–7.61 (m, 1H), 7.38–7.33 (m, 1H), 7.28–7.25 (m, 1H), 7.19 (d, 1H, J = 2.2 Hz), 6.91 (dd, 1H, J = 8.7, 2.2 Hz), 6.63–6.57 (m, 2H), 5.30 (s, 2H), 5.21 (d, 2H, J = 4.7 Hz), 2.72 (s, 3H); ^{13}C NMR (DMSO-d_6) δ 158.73, 150.59 (dd, J = 52.7,12.4 Hz), 148.16 (dd, J = 54.5,12.4 Hz), 143.01, 141.76, 141.34, 137.74, 134.58, 133.67, 131.50, 125.28, 124.55, 123.84, 123.83 (d, J = 3.1 Hz), 122.63, 117.63 (d, J = 17.2 Hz), 115.12, 115.00 (d, J = 17.4 Hz), 127.23, 111.94, 109.46, 95.82, 61.45, 51.14, 20.31; ESI-MS: *m/z* 432.2 (M+1)$^+$; Anal. Calcd. for $C_{24}H_{19}F_2N_5O$: C, 66.81; H, 4.44; N, 16.23, found: C, 66.94; H, 4.66; N, 16.47.

*4.1.9.7. 1-[(2E)-3-(4-chlorophenyl)prop-2-en-1-yl]-4-[({1-methyl-9H-pyrido[3,4-b]indol-7-yl}oxy)methyl]-1H-1,2,3-triazole (**7g**).* From the reaction of 0.043 g **2g** and 0.047 g **4** and after purification by column chromatography (mobile phase cyclohexane/ethyl acetate/methanol 1:1:0.3) and trituration with diethyl ether 0.040 g (47%) of **7g** was obtained; mp 216–218 °C; IR (KBr, ν/cm^{-1}) 3135, 3100, 3080, 2959, 2874, 2758, 1627, 1567, 1486, 1438, 1415, 1392, 1325, 1277, 1238, 1222, 1175, 1134, 1104, 1070, 1053, 1033, 1015, 969, 826, 809, 743, 695; ^{1}H NMR (DMSO-d_6) δ 11.49 (s, 1H), 8.30 (s, 1H), 8.16 (d, 1H, J = 5.3 Hz), 8.07 (d, 1H, J = 8.7 Hz), 7.82 (d, 1H, J = 5.3 Hz), 7.46 (d, 2H, J = 8.6 Hz), 7.36 (d, 2H, J = 8.6 Hz), 7.19 (d, 1H, J = 2.1 Hz), 6.91 (dd, 1H, J = 8.7, 2.2 Hz), 6.62–6.56 (m, 2H), 5.30 (s, 2H), 5.21 (d, 2H, J = 4.9 Hz), 2.73 (s, 3H); ^{13}C NMR (DMSO-d_6) δ 158.79, 143.02, 141.83, 141.30, 137.61, 134.67, 134.59, 132.52,

132.25, 128.66, 128.29, 127.23, 124.74, 124.58, 122.69, 115.11, 112.02, 109.57, 95.87, 61.47, 51.27, 20.25; ESI-MS: *m/z* 430.2 $(M+1)^+$; Anal. Calcd. for $C_{24}H_{20}ClN_5O$: C, 67.05; H, 4.69; N, 16.29, found: C, 67.17; H, 4.97; N, 16.36.

*4.1.9.8. 1-[(2E)-3-(3-bromophenyl)prop-2-en-1-yl]-4-[({1-methyl-9H-pyrido[3,4-b]indol-7-yl}oxy)methyl]-1H-1,2,3-triazole (**7h**).* From the reaction of 0.052 g **2h** and 0.047 g **4** and after purification by column chromatography (mobile phase cyclohexane/ethyl acetate/methanol 3:1:0.5) and trituration with diethyl ether 0.057 g (60%) of **7h** was obtained; mp 104–106 °C (decomp.); IR (KBr, ν/cm^{-1}) 3373, 3203, 3149, 3064, 2878, 1629, 1566, 1485, 1449, 1426, 1382, 1324, 1303, 1278, 1236, 1137, 1107, 1060, 1008, 965, 865, 809, 780, 670; ^{1}H NMR (DMSO-d_6) δ 11.52 (s, 1H), 8.30 (s, 1H), 8.16 (d, 1H, J = 5.3 Hz), 8.06 (d, 1H, J = 8.7 Hz), 7.81 (d, 1H, J = 5.3 Hz), 7.47–7.42 (m, 2H), 7.27 (t, 1H, J = 7.8 Hz), 7.19 (d, 1H, J = 2.1 Hz), 6.91 (dd, 1H, J = 8.7, 2.2 Hz), 6.63–6.62 (m, 2H), 5.30 (s, 2H), 5.22 (d, 2H, J = 4.9 Hz), 2.72 (s, 3H); ^{13}C NMR (DMSO-d_6) δ 158.75, 143.02, 141.77, 141.35, 138.28, 137.75, 134.59, 132.01, 130.75, 129.03, 127.13, 125.7,125.63, 124.57, 122.64, 122.16, 115.12, 111.96, 109.47, 95.83, 61.47, 51.22, 20.33; ESI-MS: *m/z* 474.1 $(M+1)^+$, 476.2 $(M+2+1)^+$; Anal. Calcd. for $C_{24}H_{20}BrN_5O$: C, 60.77; H, 4.25; N, 14.76, found: C, 60.99; H, 4.29; N, 14.92.

*4.1.9.9. 1-[(2E)-2-methyl-3-phenylprop-2-en-1-yl]-4-[({1-methyl-9H-pyrido[3,4-b]indol-7-yl}oxy)methyl]-1H-1,2,3-triazole (**7i**).* From the reaction of 0.038 g **2i** and 0.047 g **4** and after purification by column chromatography (mobile phase cyclohexane/ethyl acetate/methanol 3:1:0.5) and trituration with diethyl ether 0.063 g (78%) of **7i** was obtained; mp 94–96 °C; IR (KBr, ν/cm^{-1}) 3134, 3059, 2946, 2866, 1628, 1567, 1483, 1446, 1382, 1328, 1281, 1234, 1168, 1051, 1016, 942, 879, 814, 695, 670; ^{1}H NMR (DMSO-d_6) δ 11.52 (s, 1H), 8.29 (s, 1H), 8.16 (d, 1H, J = 4.6 Hz), 8.07 (d, 1H, J = 8.7 Hz), 7.83 (d, 1H, J = 5.2 Hz), 7.41–7.23 (m, 5H), 7.19 (d, 1H, J = 2.1 Hz), 6.92 (dd, 1H, J = 8.7,2.2 Hz), 6.44 (s, 1H), 5.31 (s, 2H), 5.13 (s, 2H), 2.73 (s, 3H), 1.76 (s, 3H); ^{13}C NMR (DMSO-d_6) δ 158.80, 142.98, 141.88, 141.21, 137.43, 136.32, 134.57, 132.81, 128.71, 128.39, 128.28, 127.29, 126.96, 124.88, 122.70, 115.09, 112.03, 109.65, 95.91, 61.51, 57.30, 20.17, 15.60; ESI-MS: *m/z* 410.1 $(M+1)^+$; Anal. Calcd. for $C_{25}H_{23}N_5O$: C, 73.33; H, 5.66; N, 17.10, found: C, 73.38; H, 5.81; N, 17.36.

*4.1.10. General procedure for the synthesis of N,O-bis-harmicines **8a-g,i***

N,O-bis-harmicines were prepared according to the literature procedure [35]. In short, propargyl derivative **5** (0.055 g, 0.2 mmol) and the corresponding cinnamyl azide **2a-g** or **2i** (0.44 mmol) were dissolved in methanol (6 mL) and $Cu(OAc)_2$ (0.01 mmol) was added. The reaction mixture was stirred overnight at r. t. The solvent was removed under the reduced pressure.

*4.1.10.1. 4-{[1-Methyl-7-({1-[(2E)-3-phenylprop-2-en-1-yl]-1H-1,2,3-triazol-4-yl}methoxy)-9H-pyrido[3,4-b]indol-9-yl]methyl}-1-[(2E)-3-phenylprop-2-en-1-yl]-1H-1,2,3-triazole (**8a**).* From the reaction of 0.070 g **2a** and 0.055 g **5** and after purification by column chromatography (mobile phase dichloromethane/methanol 9.5:0.5) 0.062 g (52%) of **8a** was obtained; mp 138–139 °C; IR (KBr, ν/cm^{-1}) 3194, 1630, 1562, 1450, 1422, 1328, 1278, 1216, 1172, 1052, 1008, 968, 804, 772, 692; ^{1}H NMR (DMSO-d_6) δ 8.32 (s, 1H), 8.20 (bs, 1H), 8.11–8.09 (m, 2H), 7.89 (s, 1H), 7.55 (s, 1H), 7.44–7.27 (m, 10H), 6.94 (dd, 1H, J = 8.6, 1.9 Hz), 6.67–6.38 (m, 4H), 5.89 (s, 2H), 5.32 (s, 2H), 5.21 (d, 2H, J = 6.0 Hz), 5.09 (d, 2H, J = 5.7 Hz), 3.07 (s, 3H); ^{13}C NMR (DMSO-d_6) δ 159.15, 144.01, 142.85, 142.51, 142.14, 138.05, 135.68, 133.72, 133.38, 128.68, 128.66, 128.46, 128.16, 128.08, 126.56, 126.49, 124.66, 123.74, 123.64, 123.06, 122.48, 114.72, 109.90, 95.10, 61.47, 51.38, 51.27, 39.64, 22.92; ESI-MS: *m/z* 593.3 $(M+1)^+$; Anal. Calcd. for $C_{36}H_{32}N_8O$: C, 72.95; H, 5.44; N, 18.91, found: C, 72.78; H, 5.71; N, 18.73.

*4.1.10.2. 1-[(2E)-3-(4-methoxyphenyl)prop-2-en-1-yl]-4-{[7-({1-[(2E)-3-(4-methoxyphenyl)prop-2-en-1-yl]-1H-1,2,3-triazol-4-yl}methoxy)-1-methyl-9H-pyrido[3,4-b]indol-9-yl]methyl}-1H-1,2,3-triazole (**8b**).* From the reaction of 0.084 g **2b** and 0.055 g **5** and after purification by column chromatography (mobile phase dichloromethane/methanol 9.5:0.5) 0.073 g (56%) of **8b** was obtained; mp 115–117 °C; IR (KBr, ν/cm^{-1}) 3124, 3056, 3004, 2956, 2934, 2838, 1624, 1570, 1512, 1448, 1408, 1344, 1304, 1252, 1176, 1136, 1032, 970, 810; ^{1}H NMR (DMSO-d_6) δ 8.31 (s, 1H), 8.19 (d, 1H, J = 5.2 Hz), 8.11–8.08 (m, 2H), 7.89 (d, 1H, J = 5.2 Hz), 7.56 (d, 1H, J = 1.8 Hz), 7.34 (dd, 4H, J = 13.3, 8.7 Hz), 6.94 (dd, 1H, J = 8.6, 1.9 Hz), 6.88–6.84 (m, 4H), 6.58 (d, 1H, J = 15.8 Hz), 6.49 (d, 1H, J = 15.8 Hz), 6.40–6.21 (m, 2H), 5.89 (s, 2H), 5.33 (s, 2H), 5.16 (d, 2H, J = 6.3 Hz), 5.05 (d, 2H, J = 6.3 Hz), 3.74 (s, 3H), 3.73 (s, 3H), 3.08 (s, 3H); ^{13}C NMR (DMSO-d_6) δ 159.24, 159.19, 143.91, 142.82, 142.58, 141.15, 137.85, 133.41, 133.16, 128.58, 128.28, 128.26, 127.87, 127.81, 124.51, 122.90, 122.47, 121.08, 121.02, 114.71, 114.05, 112.36, 109.99, 95.16, 61.49, 55.10, 51.48, 51.38, 39.66, 23.13; ESI-MS: *m/z* 653.4 $(M+1)^+$; Anal. Calcd. for $C_{38}H_{36}N_8O_3$: C, 69.92; H, 5.56; N, 17.17, found: C, 69.78; H, 5.66; N, 17.04.

*4.1.10.3. 1-[(2E)-3-(2H-1,3-benzodioxol-5-yl)prop-2-en-1-yl]-4-{[7-({1-[(2E)-3-(2H-1,3-benzodioxol-5-yl)prop-2-en-1-yl]-1H-1,2,3-triazol-4-yl}methoxy)-1-methyl-9H-pyrido[3,4-b]indol-9-yl]methyl}-1H-1,2,3-triazole (**8c**).* From the reaction of 0.090 g **2c** and 0.055 g **5** and after purification by column chromatography (mobile phase DCM/methanol 9.5:0.5) and trituration with diethyl ether 0.129 g (96%) of **8c** was obtained; mp 126–127 °C; IR (KBr, ν/cm^{-1}) 3122, 3068, 2900, 1624, 1566, 1504, 1446, 1406, 1344, 1252, 1172, 1124, 1038, 966, 930, 802; ^{1}H NMR (DMSO-d_6) δ 8.30 (s, 1H), 8.18 (d, 1H, J = 5.1 Hz), 8.10 (d, 1H, J = 8.6 Hz), 8.06 (s, 1H), 7.88 (d, 1H, J = 5.2 Hz), 7.55 (d, 1H, J = 1.8 Hz), 7.14 (s, 1H), 7.06 (s, 1H), 6.94 (dd, 1H, J = 8.6, 2.0 Hz), 6.84–6.77 (m, 4H), 6.57 (d, 1H, J = 15.8 Hz), 6.46 (d, 1H, J = 16.0 Hz), 6.41–6.24 (m, 2H), 6.01, 5.99 (2s, 2H), 5.89 (s, 2H), 5.32 (s, 2H), 5.16 (d, 2H, J = 6.4 Hz), 5.04 (d, 2H, J = 6.1 Hz), 3.07 (s, 3H); ^{13}C NMR (DMSO-d_6) δ 159.28, 147.91, 147.87, 147.38, 147.33, 144.06, 142.93, 142.65, 141.30, 138.09, 134.76, 133.74, 133.41, 130.23, 130.19, 128.66, 124.69, 122.95, 122.63, 121.81, 121.75, 121.70, 121.67, 114.81, 112.47, 110.09, 108.44, 108.37, 105.69, 105.66, 101.23, 101.20, 95.19, 61.54, 51.55, 51.44, 39.80, 23.26; ESI-MS: *m/z* 681.3 $(M+1)^+$; Anal. Calcd. for $C_{38}H_{32}N_8O_5$: C, 67.05; H, 4.74; N, 16.46, found: C, 67.09; H, 5.02; N, 16.20.

*4.1.10.4. 1-[(2E)-3-(3-fluorophenyl)prop-2-en-1-yl]-4-{[7-({1-[(2E)-3-(3-fluorophenyl)prop-2-en-1-yl]-1H-1,2,3-triazol-4-yl}methoxy)-1-methyl-9H-pyrido[3,4-b]indol-9-yl]methyl}-1H-1,2,3-triazole (**8d**).* From the reaction of 0.078 g **2d** and 0.055 g **5** and after purification by column chromatography (mobile phase cyclohexane/ethyl acetate/methanol 3:1:0.5) 0.047 g (37%) of **8d** was obtained; mp 162–164 °C; IR (KBr, ν/cm^{-1}) 3126, 3062, 2962, 2932, 2886, 1624, 1584, 1492, 1446, 1406, 1324, 1250, 1220, 1170, 1138, 1052, 970, 874, 788; ^{1}H NMR (DMSO-d_6) δ 8.34 (s, 1H), 8.19 (d, 1H, J = 5.2 Hz), 8.12–8.10 (m, 2H), 8.10 (s, 1H), 7.90 (d, 1H, J = 5.2 Hz), 7.57 (d, 1H, J = 1.9 Hz), 7.39–7.05 (m, 8H), 6.95 (dd, 1H, J = 8.6, 2.1 Hz), 6.64–6.62 (m, 2H), 6.54–6.52 (m, 2H), 5.91 (s, 2H), 5.33 (s, 2H), 5.22 (d, 2H, J = 4.6 Hz), 5.11 (d, 2H, J = 4.6 Hz), 3.08 (s, 3H); ^{13}C NMR (DMSO-d_6) δ 162.26, 162.21 (2d, J = 243.5 Hz), 159.19, 143.86, 142.65, 142.58, 141.15, 137.95, 134.64, 132.43, 132.08, 130.63–130.51 (2d), 128.56, 125.53, 125.42, 124.62, 124.44, 124.40, 122.98, 122.49, 115.12, 115.09, 114.88 (2d, J = 7, 6.9 Hz), 114.69, 112.88, 112.67 (2d, J = 6.3 Hz), 112.33, 109.97, 95.08, 61.51, 51.22, 51.10, 39.72, 23.16;

ESI-MS: *m/z* 629.3 $(M+1)^+$; Anal. Calcd. for $C_{36}H_{30}F_2N_8O$: C, 68.78; H, 4.81; F, 6.04; N, 17.82, found: C, 68.57; H, 5.07; N, 17.93.

*4.1.10.5. 1-[(2E)-3-(4-fluorophenyl)prop-2-en-1-yl]-4-{[7-({1-[(2E)-3-(4-fluorophenyl)prop-2-en-1-yl]-1H-1,2,3-triazol-4-yl}methoxy)-1-methyl-9H-pyrido[3,4-b]indol-9-yl]methyl}-1H-1,2,3-triazole (**8e**).* From the reaction of 0.078 g **2e** and 0.055 g **5** and after purification by column chromatography (mobile phase DCM/methanol 9.5:0.5) 0.047 g (37%) of **8e** was obtained; mp 209–210 °C; IR (KBr, ν/cm^{-1}) 3120, 3060, 2956, 1626, 1600, 1570, 1510, 1452, 1408, 1346, 1238, 1170, 1134, 1052, 1006, 962, 914, 804, 768; ^{1}H NMR (DMSO-d_6) δ 8.32 (s, 1H), 8.19 (d, 1H, J = 4.3 Hz), 8.10 (d, 1H, J = 8.6 Hz), 8.08 (s, 1H), 7.89 (d, 1H, J = 5.1 Hz), 7.55 (d, 1H, J = 2.0 Hz), 7.50–7.41 (m, 4H), 7.17–7.10 (m, 4H), 6.94 (dd, 1H, J = 8.6, 2.1 Hz), 6.63 (d, 1H, J = 15.9 Hz), 6.55–6.35 (m, 3H), 5.89 (s, 2H), 5.32 (s, 2H), 5.19 (d, 2H, J = 6.1 Hz), 5.08 (d, 2H, J = 6.1 Hz), 3.07 (s, 3H); ^{13}C NMR (DMSO-d_6) δ 161.87 (2d, J = 250.1, 240.5 Hz), 159.18, 143.98, 142.84, 142.55, 141.18, 137.95, 134.07, 132.54, 132.24, 132.30, 128.51 (t, J = 7.5 Hz), 128.44, 124.66, 123.62, 123.53, 123.04, 122.51, 115.52 (d, J = 21.6 Hz), 114.70, 112.35, 109.95, 95.11, 61.47, 51.34, 51.23, 39.79, 23.20; ESI-MS: *m/z* 629.3 $(M+1)^+$; Anal. Calcd. for $C_{36}H_{30}F_2N_8O$: C, 68.78; H, 4.81; N, 17.82, found: C, 68.89; H, 4.96; N, 17.99.

*4.1.10.6. 1-[(2E)-3-(3,4-difluorophenyl)prop-2-en-1-yl]-4-{[7-({1-[(2E)-3-(3,4-difluorophenyl)prop -2-en-1-yl]-1H-1,2,3-triazol-4-yl} methoxy)-1-methyl-9H-pyrido[3,4-b]indol-9-yl]methyl}-1H-1,2,3-triazole (**8f**).* From the reaction of 0.086 g **2f** and 0.055 g **5** and after purification by column chromatography (mobile phase cyclohexane/ethyl acetate/methanol 3:1:0.5) and trituration with diethyl ether 0.044 g (33%) of **8f** was obtained; mp 128–129 °C (decomp.); IR (KBr, ν/cm^{-1}) 3112, 3062, 1622, 1566, 1516, 1446, 1406, 1328, 1294, 1254, 1210, 1168, 1138, 1038, 1102, 966, 870, 820, 778; ^{1}H NMR (DMSO-d_6) δ 8.34 (s, 1H), 8.18 (d, J = 5.0 Hz, 1H), 8.11–8.06 (m, 2H), 7.88 (d, 1H, J = 5.0 Hz), 7.56–7.22 (m, arom. 7H), 6.94 (d, 1H, J = 8.1 Hz), 6.60–6.59 (m, 2H), 6.49–6.48 (m, 2H), 5.90 (s, 2H), 5.33 (s, 2H), 5.21 (d, 2H, J = 4.1 Hz), 5.10 (s, 2H), 3.08 (s, 3H); ^{13}C NMR (DMSO-d_6) δ159.14, 150.91–150.22 (m), 148.47–147.77 (m), 144.01, 142.85, 142.51, 141.20, 138.07, 134.65, 133.59, 131.57, 131.27, 128.48, 125.26 (d, J = 9.3 Hz), 124.71, 123.77, 123.09, 122.47, 117.61 (d, J = 17.2 Hz), 115.04 (d, J = 5.4 Hz), 114.86 (d, J = 5.4 Hz), 114.72, 112.30, 109.90, 95.10, 61.45, 51.18, 51.07, 39.73, 23.26; ESI-MS: *m/z* 665.2 $(M+1)^+$; Anal. Calcd. for $C_{36}H_{28}F_4N_8O$: C, 65.05; H, 4.25; N, 16.86, found: C, 65.27; H, 4.03; N, 16.67.

*4.1.10.7. 1-[(2E)-3-(4-chlorophenyl)prop-2-en-1-yl]-4-{[7-({1-[(2E)-3-(4-chlorophenyl)prop-2-en-1-yl]-1H-1,2,3-triazol-4-yl}methoxy)-1-methyl-9H-pyrido[3,4-b]indol-9-yl]methyl}-1H-1,2,3-triazole (**8g**).* From the reaction of 0.086 g **2g** and 0.055 g **5** and after purification by column chromatography (mobile phase cyclohexane/ethyl acetate/methanol 3:1:0.5) and trituration with diethyl ether 0.049 g (37%) of **8g** was obtained; mp 201–203 °C; IR (KBr, ν/cm^{-1}) 3122, 2964, 2886, 1624, 1568, 1492, 1448, 1406, 1326, 1252, 1218, 1172, 1134, 1094, 1052, 1010, 970, 804; ^{1}H NMR (DMSO-d_6) δ 8.34 (s, 1H), 8.19 (d, 1H, J = 5.2 Hz), 8.12–8.10 (m, 2H), 7.91 (d, 1H, J = 5.2 Hz), 7.56 (d, 1H, J = 2.0 Hz), 7.47–7.34 (m, 8H), 6.95 (dd, 1H, J = 8.6, 2.1 Hz), 6.64–6.43 (m, 4H), 5.90 (s, 2H), 5.34 (s, 2H), 5.21 (d, 2H, J = 5.4 Hz), 5.10 (d, 2H, J = 5.0 Hz), 3.09 (s, 3H); ^{13}C NMR (DMSO-d_6) δ 159.12, 144.00, 142.86, 142.50, 141.20, 138.06, 134.64, 132.52, 132.45, 132.32, 132.02, 128.63, 128.27, 128.21, 128.47, 124.76, 124.71, 124.67, 123.09, 122.47, 114.71, 112.31, 109.93, 95.11, 61.45, 51.28, 51.18, 39.73, 23.26; ESI-MS: *m/z* 661.2 $(M+1)^+$; Anal. Calcd. for $C_{36}H_{30}Cl_2N_8O$: C, 65.36; H, 4.57; N, 16.94, found: C, 65.49; H, 4.66; N, 17.10.

*4.1.10.8. 1-[(2E)-2-methyl-3-phenylprop-2-en-1-yl]-4-{[1-methyl-7-({1-[(2E)-2-methyl-3-phenyl prop-2-en-1-yl]-1H-1,2,3-triazol-4-yl} methoxy)-9H-pyrido[3,4-b]indol-9-yl]methyl}-1H-1,2,3-triazole (**8i**).* From the reaction of 0.076 g **2i** and 0.055 g **5** and after purification by column chromatography (mobile phase cyclohexane/ethyl acetate/methanol 1:1:0.5) and trituration with diethyl ether 0.096 g (77%) of **8i** was obtained; mp 87–88 °C; IR (KBr, ν/cm^{-1}) 3104, 3052, 2982, 2930, 1622, 1566, 1494, 1446, 1406, 1332, 1252, 1220, 1176, 1136, 1044, 1014, 920, 812; ^{1}H NMR (DMSO-d_6) δ 8.32 (s, 1H), 8.19 (d, 1H, J = 5.2 Hz), 8.12–8.09 (m, 2H), 7.89 (d, 1H, J = 5.2 Hz), 7.58 (d, 1H, J = 1.8 Hz), 7.34–7.17 (m, 10H), 6.95 (dd, 1H, J = 8.6, 1.9 Hz), 6.47 (s, 1H), 6.32 (s, 1H), 5.91 (s, 2H), 5.33 (s, 2H), 5.13 (s, 2H), 5.02 (s, 2H), 3.07 (s, 3H), 1.75 (s, 3H), 1.68 (s, 3H); ^{13}C NMR (DMSO-d_6) δ 159.16, 143.95, 142.81, 142.58, 141.14, 137.98, 136.30, 136.26, 134.69, 132.81, 132.71, 128.66, 128.59, 128.55, 128.25, 128.23, 128.49, 128.03, 126.93, 126.86, 124.93, 123.40, 122.41, 114.75, 112.26, 109.96, 95.22, 61.54, 57.33, 57.07, 39.66, 23.12, 15.53, 15.46; ESI-MS: *m/z* 621.4 $(M+1)^+$; Anal. Calcd. for $C_{38}H_{36}N_8O$: C, 73.53; H, 5.85; N, 18.05, found: C, 73.33; H, 5.66; N, 18.10.

4.2. In vitro drug sensitivity assay against erythrocytic stages of P. falciparum

Antiplasmodial activity of harmicines **6**–**8** was evaluated against two laboratory *P. falciparum* strains (3D7 – CQ-sensitive, and Dd2 – CQ-resistant), as previously described, using the histidine-rich protein 2 (HRP2) assay [36,37]. In brief, 96-well plates were pre-coated with the tested compounds in a three-fold dilution before ring stage parasites were added in complete culture medium at a hematocrit of 1.5% and a parasitaemia of 0.05%. After three days of incubation at 37 °C, 5% CO_2 and 5% oxygen, plates were frozen until analyzed by HRP2-ELISA. All compounds were evaluated in duplicate in at least two independent experiments. The IC_{50} was determined by analysing the nonlinear regression of log concentration-response curves using the drc-package v0.9.0 of R v2.6.1 [38].

4.3. In vitro activity against P. berghei hepatic stages

In vitro activity of harmicines **6**–**8** against the liver stage of *P. berghei* infection was assessed as previously described [40,41]. Briefly, Huh7 cells were routinely cultured in 1640 Roswell Park Memorial Institute (RPMI) medium supplemented with 10% (v/v) fetal bovine serum, 1% (v/v) glutamine, 1% (v/v) penicillin/streptomycin, 1% non-essential amino acids, and 10 mM 2-(4-(2-hydroxyethyl)piperazin-1-yl)ethanesulfonic acid (HEPES). For drug screening experiments, Huh7 cells were seeded at 1×10^4 cell/well of a 96-well plate and incubated overnight at 37 °C with 5% CO_2. 10 mM stock solutions of test compounds were prepared in DMSO and were serially diluted in infection medium, i.e. culture medium supplemented with gentamicin (50 μg/mL) and amphotericin B (0.8 μg/mL), in order to obtain the test concentrations. On the day of the infection, the culture medium was replaced by the serial dilutions of test compounds and incubated for 1 h at 37 °C with 5% CO_2. Next, 1×10^4 firefly luciferase-expressing *P. berghei* sporozoites, freshly isolated from the salivary glands of female infected *Anopheles stephensi* mosquitoes, were added to the cultures, plates were centrifuged at 1800×*g* for 5 min at room temperature and incubated at 37 °C with 5% CO_2.

To assess the effect of each compound concentration on cell viability, at 46 h post infection (hpi), cultures were incubated with Alamar Blue (Invitrogen, UK), according to the manufacturer's recommendations. Parasite load was then assessed by a bioluminescence assay (Biotium, Fremont, CA, USA), using a multi-plate reader Infinite M200 (Tecan, Switzerland). Nonlinear regression

analysis was employed to fit the normalized results of the dose-response curves, and IC_{50} values were determined using GraphPad Prism 6.0 (GraphPad software, La Jolla, CA, USA).

4.4. In vitro cytotoxicity assay

Cytotoxicity against a human cell line (HepG2) was evaluated using the neutral red assay [45]. In brief, human cells were seeded to a 96 well plate in complete culture medium, before on the following day a serial dilution of the respective compound was added. After one day incubation cytotoxicity was evaluated by addition of Neutral Red, subsequent lysis of cells and measurement of absorbance in a plate reader. The IC_{50} was determined as for the *in vitro* drug assay against *P. falciparum.* To assess the safety of a compound, SI was calculated as the fractional ratio between the IC_{50}s for human cell lines and *P. falciparum*.

4.5. Molecular dynamics simulations

The starting point of our calculations was a *Pf*Hsp90 N-terminal domain structure obtained by the X-ray crystallography from Protein data bank (accession code 3K60). Ligands (ADP and SO_4^{2-}) were removed from the model and selected compounds were placed in the ATP binding pocket, including harmine as a reference. Original crystal waters were removed from the structure so that water molecules from the bulk solvent could diffuse into the protein during equilibration and production MD runs. For investigated compounds, geometry optimisation and RESP charge calculations were performed with the Gaussian 16 program [53] at the HF/6−31G(d) level to be consistent with the employed GAFF force field, while the *Pf*Hsp90 was modeled using the AMBER ff14SB force field. Such protein complexes were solvated in a truncated octahedral box of TIP3P water molecules spanning a 10 Å thick buffer, neutralized by Na^+ ions and submitted to geometry optimisation in AMBER16 program [54], employing periodic boundary conditions in all directions. Optimized systems were gradually heated from 0 to 300 K and equilibrated during 30 ps using NVT conditions, followed by productive and unconstrained MD simulations of 300 ns employing a time step of 2 fs at a constant pressure (1 atm) and temperature (300 K), the latter held constant using Langevin thermostat with a collision frequency of 1 ps^{-1}. Bonds involving hydrogen atoms were constrained using the SHAKE algorithm [55], while the long-range electrostatic interactions were calculated employing the Particle Mesh Ewald method [56]. The nonbonded interactions were truncated at 10.0 Å.

4.5.1. Binding free energy calculations

The binding free energy, ΔG_{BIND}, of harmine and its derivatives within the PfHsp90 ATP binding site was calculated using the established MM-GBSA protocol [57,58] available in AmberTools16 [52], which is the widely used method for the binding free energy calculations from the snapshots of MD trajectory [59] with an estimated standard error of 1−3 kcal mol^{-1} [57,58]. Within this approach, ΔG_{BIND} is calculated as:

$$\Delta G_{BIND} = < G_{complex} > - < G_{HSP90} > - < G_{ligand} > \quad (1)$$

where the symbol < > represents the average value over 1000 snapshots collected from the 30 ns part of the corresponding MD trajectory where investigated compounds are equally oriented in the ADP binding site. The free energy of a system can be approximated by three terms:

$$G_{complex/protein/ligand} = E_{MM} + G_{solv} - T \cdot \Delta S_{MM} \quad (2)$$

where E_{MM}, the gas-phase molecular mechanical energy, is obtained as a sum of $E_{internal}$, E_{VDW}, and E_{elec} contributions. G_{solv}, the solvation free energy, is a sum of polar (G_{polar}) and nonpolar ($G_{nonpolar}$) components, with the former calculated by solving the finite-difference Generalized Born equation, while the latter was determined on the basis of the solvent-accessible surface area (SASA) as:

$$G_{nonpolar} = \gamma \cdot SASA + \beta \quad (3)$$

with recommended empirical parameters $\gamma = 0.0054$ kcal mol^{-1} $Å^{-2}$ and $\beta = 0.92$ kcal mol^{-1} [60]. The solute conformational entropy (S_{MM}) was estimated by the normal-mode analysis. The interior and exterior dielectric constants were set to 1 and 80, respectively [61].

4.5.2. Binding free energy decomposition

The calculated MM-GBSA binding free energies were decomposed into specific residue contribution on a per-residue basis according to established procedures [62,63], and in line with our earlier reports [64]. This protocol calculates the contributions to ΔG_{BIND} arising from each amino acid side chains and identifies the nature of the energy change in terms of interaction and solvation energies, or entropic contributions. The obtained results are usually found in fair agreements with alanine scanning experiments [62,65] and open the way to rational protein engineering.

Declaration of competing interest

The authors declare that they have no known competing financial interests or personal relationships that could have appeared to influence the work reported in this paper.

Acknowledgement

The authors acknowledge the financial support by the Croatian Science Foundation (research project UIP-2017-05-5160), University of Zagreb (support for 2018), and Fundação para a Ciência e Tecnologia, Portugal (FCT) (grant 02/SAICT/2017/29550).

Abbreviations

ADMP	2-azido-1,3-dimethyl-imidazolinium hexafluorophosphate
CAD	cinnamic acid derivative
CQ	chloroquine
CuAAC	Cu(I) catalyzed azide-alkyne cycloaddition
DBU	1,8-diazabicyclo[5.4.0]undec-7-ene
DCM	dichloromethane
ESI	electrospray ionization
ΔG_{BIND}	calculated binding free energies
HEPES	2-(4-(2-hydroxyethyl)piperazin-1-yl)ethanesulfonic acid
HepG2	human liver hepatocellular carcinoma cell line
HRP2	histidine-rich protein 2
Huh7	human hepatoma cell line
IC_{50}	the concentration of the tested compound necessary for 50% growth inhibition
log *P* −	partition coefficient
MD	molecular dynamics
*Pf*3D7	chloroquine-sensitive strain of *P. falciparum*
*Pf*Dd2	chloroquine-resistant strain of *P. falciparum*
*Pf*Hsp90	*P. falciparum* heat shock protein 90
PQ	primaquine
RPMI	Roswell Park Memorial Institute

SAR	structure-activity relationship
SASA	solvent-accessible surface area
SI	selectivity index
S_{MM}	solute conformational entropy
TMS	tetramethylsilane

Appendix A. Supplementary data

Supplementary data to this article can be found online at https://doi.org/10.1016/j.ejmech.2019.111927.

References

[1] World malaria report 2017, accessed 15 July 2019, http://www.who.int/malaria/publications/world-malaria-report-2018/report/en/, 2018.
[2] C. Teixeira, N. Vale, B. Pérez, A. Gomes, J.R. Gomes, "Recycling" classical drugs for malaria, Chem. Rev. 114 (2014) 11164–11220.
[3] D. Shahinas, A. Folefoc, D.R. Pillai, Targeting *Plasmodium falciparum* Hsp 90: towards reversing antimalarial resistance, Pathogens 2 (2013) 33–54.
[4] D. Agrawal, R.D. Gupta, S.K. Awasthi, Are antimalarial hybrid molecules a close reality or a distant dream? Antimicrob. Agents Chemother. 61 (2017) e00249–17.
[5] S. Noel, S. Sharma, R. Shankar, S.K. Rath, Identification of differentially expressed genes after acute exposure to bulaquine (CDRI 80/53) in mice liver, Basic Clin. Pharmacol. Toxicol. 103 (2008) 522–529.
[6] M.V.G. Lacerda, A. Llanos-Cuentas, S. Krudsood, C. Lon, D.L. Saunders, R. Mohammed, D. Yilma, D. Batista Pereira, F.E.J. Espino, R.Z. Mia, R. Chuquiyauri, F. Val, M. Casapía, W.M. Monteiro, M.A.M. Brito, M.R.F. Costa, N. Buathong, H. Noedl, E. Diro, S. Getie, K.M. Wubie, A. Abdissa, A. Zeynudin, C. Abebe, M.S. Tada, F. Brand, H.P. Beck, B. Angus, S. Duparc, J.P. Kleim, L.M. Kellam, V.M. Rousell, S.W. Jones, E. Hardaker, K. Mohamed, D.D. Clover, K. Fletcher, J.J. Breton, C.O. Ugwuegbulam, J.A. Green, G.C.K.W. Koh, Single-dose tafenoquine to prevent relapse of *Plasmodium vivax* malaria, N. Engl. J. Med. 380 (2019) 215–228.
[7] K.E. Lyke, Steady progress toward a malaria vaccine, Curr. Opin. Infect. Dis. 30 (2017) 463–470.
[8] A. Gomes, M. Machado, L. Lobo, F. Nogueira, M. Prudêncio, C. Teixeira, P. Gomes, *N*-cinnamoylation of antimalarial classics: effects of using acyl groups other than cinnamoyl toward dual-stage antimalarials, ChemMedChem 10 (2015) 1344–1349.
[9] R. Cao, Q. Chen, X. Hou, H. Chen, H. Guan, Y. Ma, W. Peng, A. Xu, Synthesis, acute toxicities, and antitumor effects of novel 9-substituted β-carboline derivatives, Bioorg. Med. Chem. 12 (2004) 4613–4623.
[10] Q. Chen, C. Rihui, H. Chen, X. Hou, H. Yan, S. Zhou, W. Peng, A. Xu, Antitumor and neurotoxic effects of novel harmine derivatives and structure-activity relationship analysis, Int. J. Cancer 114 (2004) 675–682.
[11] D. Shahinas, G. Macmullin, C. Benedict, I. Crandall, D.R. Pillai, Harmine is a potent antimalarial targeting Hsp90 and synergises with chloroquine and artemisinin, Antimicrob. Agents Chemother. 56 (2012) 4207–4213.
[12] D. Shahinas, M. Liang, A. Datti, D.R. Pillai, A repurposing strategy idnetifies novel synergistic inhibitors of Plasmodium falciparum heat shock protein 90, J. Med. Chem. 53 (2010) 3552–3557.
[13] K.K.H. Ang, M.J. Holmes, T. Higa, M.T. Hamann, U.A.K. Kara, In vivo antimalarial activity of the beta-carboline alkaloid manzamine A, Antimicrob. Agents Chemother. 44 (2000) 1645–1649.
[14] K.L. Chan, M.J. Oneill, J.D. Phillipson, D.C. Warhurst, Plants as sources of antimalarial drugs. Part 3 1 Eurycoma longifolia, Planta Med. 2 (1986) 105–107.
[15] M. Rottmann, C. McNamara, B.K. Yeung, M.C. Lee, B. Zou, B. Russell, P. Seitz, D.M. Plouffe, N.V. Dharia, J. Tan, S.B. Cohen, K.R. Spencer, G.E. González-Páez, S.B. Lakshminarayana, A. Goh, R. Suwanarusk, T. Jegla, E.K. Schmitt, H.P. Beck, R. Brun, F. Nosten, L. Renia, V. Dartois, T.H. Keller, D.A. Fidock, E.A. Winzeler, T.T. Diagana, Spiroindolones, a potent compound class for the treatment of malaria, Science 329 (2010) 1175–1180.
[16] S.E. Huskey, C.Q. Zhu, A. Fredenhagen, J. Kühnöl, A. Luneau, Z. Jian, Z. Yang, Z. Miao, F. Yang, J.P. Jain, G. Sunkara, J.B. Mangold, D.S. Stein, KAE609 (Cipargamin), a new spiroindolone agent for the treatment of malaria: evaluation of the absorption, distribution, metabolism, and excretion of a single oral 300-mg dose of KAE609 in healthy male subjects, Drug Metab. Dispos. 44 (2016) 672–682.
[17] A.G. Bayih, A. Folefoc, A.N. Mohon, S. Eagon, M. Anderson, D.R. Pillai, In vitro and in vivo antimalarial activity of novel harmine-analog heat shock protein 90 inhibitors: a possible partner for artemisinin, Malar. J. 15 (2016) 579–590.
[18] R. Brokamp, B. Bergmann, I.B. Müller, S. Bienz, Stereoselective preparation of pyridoxal 1,2,3,4-tetrahydro-β-carboline derivatives and the influence of their absolute and relative configuration on the proliferation of the malaria parasite *Plasmodium falciparum*, Bioorg. Med. Chem. 22 (2014) 1832–1837.
[19] V. Gorki, R. Singh, N.S. Walter, U. Bagai, D.B. Salunke, Synthesis and evaluation of antiplasmodial efficacy of β-carboline derivatives against murine malaria, ACS Omega 3 (2018) 13200–13210.
[20] A. Gellis, A. Dumètre, G. Lanzada, S. Hutter, E. Ollivier, P. Vanelle, N. Azas, Preparation and antiprotozoal evaluation of promising β-carboline alkaloids, Biomed. Pharmacother. 66 (2012) 339–347.
[21] D. Pierrot, V. Sinou, S.S. Bun, D. Parzy, N. Taudon, J. Rodriguez, E. Ollivier, D. Bonne, Design and synthesis of simplified speciophylline analogues and β-carbolines as active molecules against Plasmodium falciparum, Drug Dev. Res. 80 (2019) 133–137.
[22] M. Ghavami, E.F. Merino, Z.K. Yao, R. Elahi, M.E. Simpson, M.L. Fernández-Murga, J.H. Butler, M.A. Casasanta, P.M. Krai, M.M. Totrov, D.J. Slade, P.R. Carlier, M.B. Cassera, Biological studies and target engagement of the 2-C-methyl-d-erythritol 4-phosphate cytidylyltransferase (IspD)-targeting antimalarial agent (1*R*,3*S*)-MMV008138 and analogs, ACS Infect. Dis. 4 (2018) 549–559.
[23] K. Takasu, T. Shomogama, C. Saiin, H.-S. Kim, Y. Wataya, R. Brun, M. Ihara, Synthesis and evaluation of β-carbolinium cations as new antimalarial agents based on π-delocalizes lipophilic cation (DLC) hypothesis, Chem. Pharm. Bull. 53 (2005) 653–661.
[24] M.J. Thompson, J.C. Louth, S.M. Little, M.P. Jackson, Y. Boursereau, B. Chen, I. Coldham, Synthesis and evaluation of 1-amino-6-halo-β-carbolines as antimalarial and antiprion agents, ChemMedChem 7 (2012) 578–586.
[25] Y. Boursereau, I. Coldham, Synthesis and biological studies of 1-amino β-carbolines, Bioorg. Med. Chem. Lett 14 (2004) 5841–5844.
[26] D. Barbaras, M. Kaiser, R. Brun, K. Gademann, Potent and selective antiplasmodial activity of the cyanobacterial alkaloid nostocarboline and its dimmers, Bioorg. Med. Chem. Lett 18 (2008) 4413–4415.
[27] F.W. Muregi, A. Ishih, Next-generation antimalarial drugs: hybrid molecules as a new strategy in drug design, Drug Dev. Res. 71 (2010) 20–32.
[28] R. Oliveira, D. Miranda, J. Magalhaes, R. Capela, M.J. Perry, P.M. O'Neill, R. Moreira, F. Lopes, From hybrid compounds to targeted drug delivery in antimalarial therapy, Bioorg. Med. Chem. 23 (2015) 5120–5130.
[29] B. Pérez, C. Teixeira, I.S. Albuquerque, J. Gut, P.J. Rosenthal, M. Prudêncio, P. Gomes, PRIMACINS, *N*-cinnamoyl-primaquine conjugates, with improved liver-stage antimalarial activity, Med. Chem. Commun. 3 (2012) 1170–1172.
[30] B.C. Pérez, C. Teixeira, M. Figueiras, J. Gut, P.J. Rosenthal, J.R.B. Gomes, P. Gomes, Novel cinnamic acid/4-aminoquinoline conjugates bearing non-proteinogenic amino acids: towards the development of potential dual action antimalarials, Eur. J. Med. Chem. 54 (2012) 887–899.
[31] B.C. Pérez, C. Teixeira, I.S. Albuquerque, J. Gut, P.J. Rosenthal, J.R.B. Gomes, M. Prudêncio, P. Gomes, *N*-cinnamoylated chloroquine analogues as dual-stage antimalarial leads, J. Med. Chem. 56 (2013) 556–567.
[32] B. Pérez, C. Teixeira, A.S. Gomes, I.S. Albuquerque, J. Gut, P.J. Rosenthal, M. Prudêncio, P. Gomes, In vitro efficiency of 9-(*N*-cinnamoylbutyl)amino-acridines against blood- and liver-stage malaria parasites, Bioorg. Med. Chem. Lett 23 (2013) 610–613.
[33] E. Bonandi, M.S. Christodoulou, G. Fumagalli, D. Perdicchia, G. Rastelli, D. Passarella, The 1,2,3-triazole ring as a bioisostere in medicinal chemistry, Drug Discov. Today 22 (2017) 1572–1581.
[34] M. Kitamura, T. Koga, M. Yano, T. Okauchi, Direct synthesis of organic azides from alcohols using 2-azido-1,3-dimethylimidazolinium hexafluorophosphate, Synlett 23 (2012) 1335–1338.
[35] M. Tireli, S. Maračić, S. Lukin, M. Juribašić Kulcsár, D. Žilić, M. Cetina, I. Halasz, S. Raić-Malić, K. Užarević, Solvent-free copper-catalyzed click chemistry for the synthesis of *N*-heterocyclic hybrids based on quinoline and 1,2,3-triazole, Beilstein J. Org. Chem. 13 (2017) 2352–2363.
[36] J. Held, T. Gebru, M. Kalesse, R. Jansen, K. Gerth, R. Müller, B. Mordmüller, Antimalarial activity of the myxobacterial macrolide chlorotonil a, Antimicrob. Agents Chemother. 58 (2014) 6378–6384.
[37] H. Noedl, J. Bronnert, K. Yingyuen, B. Attlmayr, H. Kollaritsch, M. Fukuda, Simple histidine-rich protein 2 double-site sandwich enzyme-linked immunosorbent assay for use in malaria drug sensitivity testing, Antimicrob. Agents Chemother. 49 (2005) 3575–3577.
[38] R Core Team, A language and environment for statistical computing. R foundation for statistical computing, Vienna, Austria, available from: https://www.R-project.org/. accessed 15 April 2019.
[39] https://chemicalize.com accessed 15 April 2019.
[40] M. Machado, M. Sanches-Vaz, J.P. Cruz, A.M. Mendes, M. Prudêncio, Inhibition of *Plasmodium* hepatic infection by antiretroviral compounds, Front. Cell. Infect. Microbiol. 7 (2017) 329.
[41] I.H.J. Ploemen, M. Prudêncio, B.G. Douradinha, J. Ramesar, J. Fonager, G.-J. van Gemert, A.J.F. Luty, C.C. Hermsen, R.W. Sauerwein, F.G. Baptista, M.M. Mota, A.P. Waters, I. Que, C.W.G.M. Lowik, S.M. Khan, C.J. Janse, B. Franke-Fayard, Visualisation and quantitative analysis of the rodent malaria liver stage by real time imaging, PLoS One 4 (2009), e7881.
[42] M. Beus, D. Fontinha, J. Held, Z. Rajić, L. Uzelac, M. Kralj, M. Prudêncio, B. Zorc, Primaquine and chloroquine fumardiamides as promising antiplasmodial agents, Molecules 24 (2019), E2812 pii.
[43] M.P. Carrasco, M. Machado, L. Gonçalves, M. Sharma, J. Gut, A.K. Lukens, D.F. Wirth, V. André, M.T. Duarte, R.C. Guedes, D. Dos Santos, P.J. Rosenthal, R. Mazitschek, M. Prudêncio, R. Moreira, Probing the Azaaurone scaffold against the hepatic and erythrocytic stages of malaria parasites, ChemMedChem 11 (2016) 2194–2204.
[44] R. Capela, J. Magalhães, D. Miranda, M. Machado, M. Sanches-Vaz, I.S. Albuquerque, M. Sharma, J. Gut, P.J. Rosenthal, R. Frade, M.J. Perry, R. Moreira, M. Prudêncio, F. Lopes, Endoperoxide-8-aminoquinoline hybrids as dual-stage antimalarial agents with enhanced metabolic stability, Eur. J. Med. Chem. 149 (2018) 69–78.

[45] E. Borenfreund, A. Puerner, A simple quantitative procedure using monolayer cultures for cytotoxicity assays (Htd/Nr-90), J. Tissue Cult. Methods 9 (1984) 7–9.
[46] D. Shahinas, G. Macmullin, C. Benedict, I. Crandall, D.R. Pillai, Harmine is a potent antimalarial targeting Hsp90 and synergises with chloroquine and artemisinin, Antimicrob. Agents Chemother. 56 (2012) 4207–4213.
[47] D. Shahinas, M. Liang, A. Datti, D.R. Pillai, A repurposing strategy idnetifies novel synergistic inhibitors of Plasmodium falciparum heat shock protein 90, J. Med. Chem. 53 (2010) 3552–3557.
[48] L.H. Pearl, C. Prodromou, Structure and mechanism of the Hsp90 molecular chaperone machinery, Annu. Rev. Biochem. 75 (2006) 271–294.
[49] M.M. Ali, S.M. Roe, C.K. Vaughan, P. Meyer, B. Panaretou, P.W. Piper, C. Prodromou, L.H. Pearl, Crystal structure of an Hsp90-nucleotide-p23/Sba1 closed chaperone complex, Nature 440 (2006) 1013–1017.
[50] K.D. Corbett, J.M. Berger, Structure of the ATP-binding domain of *Plasmodium falciparum* Hsp90, Proteins 78 (2010) 2738–2744.
[51] S.M. Roe, C. Prodromou, R. O'Brien, J.E. Ladbury, P.W. Piper, L.H. Pearl, Structural basis for inhibition of the Hsp90 molecular chaperone by the antitumor antibiotics radicicol and geldanamycin, J. Med. Chem. 42 (1999) 260–266.
[52] R. Frederick, C. Bruyere, C. Vancraeynest, J. Reniers, C. Meinguet, L. Pochet, A. Backlund, B. Masereel, R. Kiss, J. Wouters, Novel trisubstituted harmine derivatives with original in vitro anticancer activity, J. Med. Chem. 55 (2012) 6489–6501.
[53] Gaussian 16, Revision C.01, M.J. Frisch, G.W. Trucks, H.B. Schlegel, G.E. Scuseria, M.A. Robb, J.R. Cheeseman, G. Scalmani, V. Barone, G.A. Petersson, H. Nakatsuji, X. Li, M. Caricato, A.V. Marenich, J. Bloino, B.G. Janesko, R. Gomperts, B. Mennucci, H.P. Hratchian, J.V. Ortiz, A.F. Izmaylov, J.L. Sonnenberg, D. Williams-Young, F. Ding, F. Lipparini, F. Egidi, J. Goings, B. Peng, A. Petrone, T. Henderson, D. Ranasinghe, V.G. Zakrzewski, J. Gao, N. Rega, G. Zheng, W. Liang, M. Hada, M. Ehara, K. Toyota, R. Fukuda, J. Hasegawa, M. Ishida, T. Nakajima, Y. Honda, O. Kitao, H. Nakai, T. Vreven, K. Throssell, J.A. Montgomery Jr., J.E. Peralta, F. Ogliaro, M.J. Bearpark, J.J. Heyd, E.N. Brothers, K.N. Kudin, V.N. Staroverov, T.A. Keith, R. Kobayashi, J. Normand, K. Raghavachari, A.P. Rendell, J.C. Burant, S.S. Iyengar, J. Tomasi, M. Cossi, J.M. Millam, M. Klene, C. Adamo, R. Cammi, J.W. Ochterski, R.L. Martin, K. Morokuma, O. Farkas, J.B. Foresman, D.J. Fox, Gaussian, Inc., Wallingford CT, 2016.
[54] D.A. Case, R.M. Betz, D.S. Cerutti, T.E. Cheatham, T.A. Darden, R.E. Duke, T.J. Giese, H. Gohlke, A.W. Goetz, N. Homeyer, S. Izadi, P. Janowski, J. Kaus, A. Kovalenko, T.S. Lee, S. LeGrand, P. Li, C. Lin, T. Luchko, R. Luo, B. Madej, D. Mermelstein, K.M. Merz, G. Monard, H. Nguyen, H.T. Nguyen, I. Omelyan, A. Onufriev, D.R. Roe, A. Roitberg, C. Sagui, C.L. Simmerling, W.M. Botello-Smith, J. Swails, R.C. Walker, J. Wang, R.M. Wolf, X. Wu, L. Xiao, P.A. Kollman, University of California, San Francisco, 2016.
[55] J.P. Ryckaert, G. Ciccotti, H.J. Berendsen, Numerical-integration of cartesian equations of motion of a system with constraints – molecular-dynamics of N-alkanes, J. Comput. Phys. 23 (1977) 327–341.
[56] T. Darden, D. York, L.J. Pedersen, Particle mesh Ewald: an Nlog(N) method for Ewald sums in large systems, Chem. Phys. 98 (1993) 10089–10092.
[57] S. Genheden, U. Ryde, The MM/PBSA and MM/GBSA methods to estimate ligand binding affinities, Expert Opin. Drug Discov. 10 (2015) 449–461.
[58] T. Hou, J. Wang, Y. Li, W. Wang, Assessing the performance of the MM/PBSA and MM/GBSA methods. 1. The accuracy of binding free energy calculations based on molecular dynamics simulations, J. Chem. Inf. Model. 51 (2011) 69–82.
[59] G.G. Ferenczy, in: G.M. Keserü, D.C. Swinney (Eds.), Thermodynamics and Kinetics of Drug Binding, Wiley, Weinheim, 2015, pp. 37–61.
[60] P.A. Kollman, I. Massova, C. Reyes, B. Kuhn, S. Huo, L. Chong, M. Lee, T. Lee, Y. Duan, W. Wang, O. Donini, P. Cieplak, J. Srinivasan, D.A. Case, Calculating structures and free energies of complex molecules: combining molecular mechanics and continuum models, Acc. Chem. Res. 33 (2000) 889–897.
[61] D. Bashford, D.A. Case, Generalized born models of macromolecular solvation effects, Annu. Rev. Phys. Chem. 51 (2000) 129–152.
[62] H. Gohlke, C. Kiel, D.A. Case, Insights into protein-protein binding by binding free energy calculation and free energy decomposition for the Ras-Raf and Ras-RalGDS complexes, J. Mol. Biol. 330 (2003) 891–913.
[63] G. Rastelli, A. Del Rio, G. Degliesposti, M. Sgobba, Fast and accurate predictions of binding free energies using MM-PBSA and MM-GBSA, J. Comput. Chem. 31 (2010) 797–810.
[64] T. Tandarić, R. Vianello, Computational insight into the mechanism of the irreversible inhibition of monoamine oxidase enzymes by the anti-parkinsonian propargylamine inhibitors rasagiline and selegiline, ACS Chem. Neurosci. 10 (2019) 3532–3542.
[65] V. Lafont, M. Schaefer, R.H. Stote, D. Altschuh, A. Dejaegere, Protein-protein recognition and interaction hot spots in an antigen-antibody complex: free energy decomposition identifies "efficient amino acids", Proteins 67 (2007) 418–434.